

# ASGO: Adaptive Structured Gradient Optimization

Kang An<sup>1\*</sup>, Yuxing Liu<sup>2\*</sup>, Rui Pan<sup>2</sup>, Yi Ren<sup>3</sup>, Shiqian Ma<sup>1</sup>, Donald Goldfarb<sup>4</sup>, Tong Zhang<sup>2</sup>

<sup>1</sup>Rice University <sup>2</sup>University of Illinois Urbana-Champaign

<sup>3</sup>Meta Platforms, Inc. <sup>4</sup>Columbia University

{kang.an, shiqian.ma}@rice.edu, {yuxing6, ruip4, tozhang}@illinois.edu, yiren94@meta.com, goldfarb@columbia.edu

## Abstract

Training deep neural networks is a structured optimization problem, because the parameters are naturally represented by matrices and tensors rather than by vectors. Under this structural representation, it has been widely observed that gradients are low-rank and Hessians are approximately block-wise diagonal. These structured properties are crucial for designing efficient optimization algorithms, but are not utilized by many current popular optimizers like Adam. In this paper, we present a novel optimization algorithm ASGO that capitalizes on these properties by employing a preconditioner that is adaptively updated using structured gradients. By fine-grained theoretical analysis, ASGO is proven to achieve superior convergence rates compared to existing structured gradient methods. Based on the convergence theory, we further demonstrate that ASGO can benefit from the low-rank and block-wise diagonal properties. We also discuss practical modifications of ASGO and empirically verify ASGO’s effectiveness on language model tasks.

## 1 Introduction

Numerical optimization algorithms, especially those can efficiently train large foundation models [Devlin et al., 2018, Brown et al., 2020, Touvron et al., 2023, Touvron et al., Ouyang et al., 2022], play an important role in the modern machine learning field. Among them, adaptive gradient methods like AdaGrad [Duchi et al., 2011] and Adam [Kingma and Ba, 2014] are popular choices, gaining huge success in training state-of-the-art models in many tasks. These algorithms typically apply a diagonal matrix preconditioner to the gradient  $g_t$  to update the deep neural network (DNN) parameters  $w_t$ ;

$$w_{t+1} = w_t - \eta_t \Lambda_t^{-1} g_t, \text{ where } w_t \in \mathbb{R}^d, g_t \in \mathbb{R}^d, \text{ and } \Lambda_t \in \mathbb{R}^{d \times d} \text{ is a diagonal matrix.}$$

This coordinate-wise step size design has been theoretically verified to be effective as it can exploit the sparsity of the gradient vectors  $g_t$  [Duchi et al., 2011]. Also, when the Hessian is well-approximated by a diagonal matrix whose diagonal entries have very different scales, adaptive gradient methods have been proven to be beneficial [Liu et al., 2024, Jiang et al., 2024a, Xie et al., 2024]. While these results seem to be convincing, common DNNs do not necessarily have sparse gradients or Hessians that are well-approximated by ill-conditioned diagonal matrices. Instead, if we take the matrix structure of gradients in neural networks into account, it has been widely observed that these structured gradients are usually low-rank [Zhao et al., 2021, Yang et al., 2023, Cosson et al., 2023], and the Hessians are well-approximated by block-wise diagonal matrices [Collobert, 2004, Zhang et al., 2024a,b]. Since adaptive gradient methods like Adam, treat the parameters as vectors and ignore the matrix structure of gradients, they are generally unable to exploit these structured properties. This gap makes us ask the following question: *How can we properly consider the matrix structures of gradients and exploit their low-rank and block-wise diagonal properties?*

One possible answer is provided by Shampoo [Gupta et al., 2018]:

$$W_{t+1} = W_t - \eta_t L_t^{-\frac{1}{4}} G_t R_t^{-\frac{1}{4}}, \text{ where } W_t, G_t \in \mathbb{R}^{m \times n} \text{ and } L_t \in \mathbb{R}^{m \times m}, R_t \in \mathbb{R}^{n \times n} \text{ are full matrices.}$$

---

\*Equal Contribution. Ordering for the first two authors is determined by a coin flip.

The main motivation for such a design is that if we apply vectorization to the update, the Shampoo preconditioner is a single matrix that is the Kronecker product of  $L_t^{-\frac{1}{4}}$  and  $R_t^{-\frac{1}{4}}$ , which approximates the full-matrix preconditioner for AdaGrad [Duchi et al., 2011]. However, the theoretical convergence of Shampoo is worse than that for AdaGrad or even SGD when the dimension is large. Also, Shampoo needs more memory and much heavier computation than adaptive gradient methods because it requires two preconditioners, making it less suitable for training large-scale DNNs.

In this paper, we provide an answer to the aforementioned question by proposing ASGO (Adaptive Structured Gradient Optimization), which significantly improves the convergence guarantees of Shampoo while requiring less memory and computation. In light of the analysis that demonstrates the benefits of adaptive gradient methods [Duchi et al., 2011, Liu et al., 2024, Jiang et al., 2024a, Xie et al., 2020], we use appropriate assumptions to enable a more fine-grained convergence analysis, showing superior convergence results and how ASGO can benefit from the low-rank and block-wise diagonal properties of the problem. We also discuss the connection between ASGO and Muon [Jordan et al., 2024], a structured gradient method based upon the steepest descent algorithm with spectral norm, to conjecture a relation between ASGO and Muon analogous to the relation between AdaGrad and SignSGD [Bernstein et al., 2018, Kunstner et al., 2023]. Furthermore, we develop an efficient design for query-key attention parameters in transformer models and examine the empirical performance on pretraining transformer model tasks. Our main contributions are summarized as follows.

- We propose the structured gradient based algorithm ASGO, theoretically analyze its convergence, and show that it converges faster than full-matrix AdaGrad and Shampoo.
- We further demonstrate that ASGO can effectively exploit the low-rankness of gradients as well as the approximate block-wise diagonal property of Hessians that is typically observed in training DNNs, hence indicating great potential of ASGO for real-world applications.
- We develop a practical implementation of ASGO with targeted modifications for transformer architectures that offers significant advantages: it eliminates the need for a separate optimizer for 1D parameters in contrast to Muon, while requiring less memory and computational complexity than Shampoo.
- We empirically validate the effectiveness of ASGO with modifications on language model tasks, demonstrating the algorithm’s great potential in real applications.

## 2 Related Work

**Adaptive Gradient Methods.** Adaptive gradient methods that use diagonal preconditioners to speedup the convergence are extremely popular for solving many real-world optimization problems. To the best of our knowledge, the first method of this kind for machine learning, AdaGrad [Duchi et al., 2011, Streeter and McMahan, 2010], was developed based on rigorous theory that showed the benefits of using this kind of preconditioner. Adam [Kingma and Ba, 2014, Loshchilov and Hutter, 2017] modified AdaGrad and has become the default choice for training large foundation models. In theory, it has been proven that adaptive gradient methods can benefit from sparse gradients and approximately ill-conditioned Hessians [Duchi et al., 2011, Liu et al., 2024, Jiang et al., 2024a, Xie et al., 2024]. It is worth noting that the original AdaGrad paper [Duchi et al., 2011] also proposed a version of AdaGrad that uses a full-matrix preconditioner instead of the diagonal one, which is believed to perform even better. However, this full-matrix AdaGrad method suffers from large memory costs for storing the preconditioner, and there is no better convergence guarantee compared to diagonal AdaGrad and SGD under the same settings as listed in Section 4.

**Optimization with Matrix Structure.** In the standard optimization literature (i.e., excluding areas such as conic optimization), it is common to consider variables as vectors. However, recently, optimization methods for machine learning that consider variables as matrices have been rapidly gaining attention. Adafactor [Shazeer and Stern, 2018], LAMB [You et al., 2019], and Adam-mini [Zhang et al., 2024b] consider the matrix or layer structure to help reduce the memory cost of Adam and enable more efficient training. Shampoo [Gupta et al., 2018] and KFAC [Martens and Grosse, 2015] are two pioneering works that approximate, respectively, the full-matrix preconditioner of AdaGrad and the

**true** Fisher matrix (FM), using Kronecker products of smaller matrices, making the memory cost more affordable. Unfortunately, the analysis in [Gupta et al., 2018] shows that the rate of convergence for Shampoo is no better than that for the full-matrix AdaGrad. We note that there is another method, TNT [Ren and Goldfarb, 2021] that is very closely related to Shampoo. TNT was developed as a natural gradient method, approximating the **true** FM by the covariance of block-wise sampling-based gradients assuming that they are Tensor-Normally distributed. The main difference between TNT and Shampoo, is that TNT uses true FMs and inverses of their Kronecker factors, whereas Shampoo uses empirical FMs and the  $-1/4$  power of their factors. More discussion on recent and concurrent work is presented in Appendix A.

### 3 Our ASGO Algorithm

#### 3.1 Notation and problem setting

Throughout this paper, we use capital letters such as  $W$  to represent matrices and  $[W]_{i,j}$  to denote the  $(i, j)$ -th entry of  $W$ . For an arbitrary matrix  $W \in \mathbb{R}^{m \times n}$ , we denote

- $\|W\|_{\text{op}}$  as the spectral norm of a matrix  $W$ , i.e., the largest singular value of it;
- $\|W\|_*$  as the trace norm of a matrix  $W$ , i.e., the summation of its singular values, which is well-known as the dual norm of the spectral norm;
- $\|W\|_F$  as the Frobenius norm of  $W$ , which also equals  $\text{tr}(W^\top W)$ , where  $\text{tr}(\cdot)$  is the trace;
- $\|W\|_L \triangleq \text{tr}(W^\top L W)$ , where  $L \in \mathbb{R}^{m \times m}$  is a real symmetric positive definite matrix.

For symmetric square matrices,  $A, B \in \mathbb{R}^{m \times m}$ ,  $A \preceq B$  denotes that  $B - A$  is positive semidefinite and  $A \prec B$  denotes that  $B - A$  is positive definite.  $\succ$  and  $\succeq$  are defined accordingly. We study the following stochastic optimization problem:

$$\min_{W \in \mathbb{R}^{m \times n}} f(W) \triangleq \mathbb{E}_\xi [f(W, \xi)], \quad (1)$$

where we only have access to a stochastic gradient oracle  $\nabla f(W; \xi)$  at  $W$ .

#### 3.2 ASGO (Algorithm 1)

We propose ASGO (**A**daptive **S**tructured **G**radient **O**ptimization) in Algorithm 1, which is an algorithm with a single-side preconditioner. Compared to full-matrix AdaGrad, ASGO preserves and utilizes the matrix structure of  $W_t$  and  $G_t$ , avoiding the huge memory cost for storing its preconditioner. ASGO's preconditioner consists of a single matrix compared to the two matrices used by Shampoo, leading to the following main update rule:

$$W_{t+1} = W_t - \eta_t V_t^{-\frac{1}{2}} G_t, \text{ where } W_t \in \mathbb{R}^{m \times n} \text{ and } V_t \in \mathbb{R}^{m \times m} \text{ is a full matrix.}$$

ASGO only needs to store one preconditioner matrix and compute its matrix square root and inverse on each iteration, versus two matrices for Shampoo. On the other hand, ASGO's preconditioner may not be as good an approximation to the full-matrix AdaGrad preconditioner or the empirical Fisher matrix [Gupta et al., 2018, Morwani et al., 2024] as Shampoo's. However, as we shall see in the following sections, this design can actually better exploit the low-rankness of gradients and the block-wise diagonal nature of Hessians, in terms of achieving better convergence rates.

### 4 Nonsmooth Theory

Although DNNs are generally nonconvex globally, convexity may apply locally in some regions. Thus, convex analysis can be helpful for understanding the behavior of DNN training algorithms.

**Assumption 1** (Convexity).  *$f(\cdot)$  is convex and  $W_*$  is one of its minimizers.*

---

**Algorithm 1** ASGO (Adaptive Structured Gradient Optimization)

---

- 1: **Input:**  $W_0 \in \mathbb{R}^{m \times n}$ , schedule  $\{\eta_t\}$  batch size  $M \in \mathbb{N}$ , and the number of iterations  $T$ ,  
 $\epsilon > 0$ , ( $\epsilon$  should be small, similar to the  $\epsilon$  for Adam or AdaGrad.)
  - 2: Initialize  $V_{-1} = 0 \in \mathbb{R}^{m \times m}$
  - 3: **for**  $t = 0$  **to**  $T - 1$  **do**
  - 4:   Sample mini-batch  $\mathcal{B}_t$  with  $|\mathcal{B}_t| \equiv M$  uniformly
  - 5:    $G_t = \frac{1}{M} \sum_{\xi \in \mathcal{B}_t} \nabla_W f(W_t; \xi)$
  - 6:    $V_t = V_{t-1} + G_t G_t^\top$
  - 7:    $\Lambda_t = V_t^{\frac{1}{2}} + \epsilon I_m$
  - 8:    $W_{t+1} = W_t - \eta_t \Lambda_t^{-1} G_t$
  - 9: **end for**
- 

**Theorem 1** (Nonsmooth convergence). *Under Assumption 1, for Algorithm 1 with  $\eta_t \equiv \eta = D_{\text{op}}$ , it holds that*

$$\frac{1}{T} \sum_{t=0}^{T-1} \mathbb{E}[f(W_t)] - f(W_*) \leq \frac{1}{T} \mathbb{E} \left[ \left\| \left( \sum_{t=0}^{T-1} G_t G_t^\top \right)^{\frac{1}{2}} \right\|_* \right] \cdot D_{\text{op}} + \frac{\epsilon D_F^2}{D_{\text{op}} T},$$

where  $D_{\text{op}} \triangleq \max_{0 \leq t \leq T-1} \|W_t - W_*\|_{\text{op}}$  and  $D_F \triangleq \max_{0 \leq t \leq T-1} \|W_t - W_*\|_F$ .

**Corollary 2.** *If we also assume an upper bound for each stochastic sub-gradient such that  $\mathbb{E}[G_t G_t^\top] \preceq Q^2$ , where  $Q \in \mathbb{R}^{m \times m}$  is a positive definite matrix, Theorem 1 also implies*

$$\frac{1}{T} \sum_{t=0}^{T-1} \mathbb{E}[f(W_t)] - f(W_*) \leq \mathcal{O} \left( \frac{\|Q\|_* D_{\text{op}}}{\sqrt{T}} + \frac{\epsilon D_F^2}{D_{\text{op}} T} \right).$$

**Remark 1.** *Note that we treat  $D_{\text{op}}$  as a constant here, but it may increase as the iteration number  $T$  increases. This can be addressed, for example, by invoking a projection onto a bounded convex set  $\mathcal{W}$  with respect to the norm  $\|\cdot\|_{\Lambda_t}$  in each iteration, as in AdaGrad [Duchi et al., 2011].  $D_{\text{op}}$  would then be bounded by the spectral norm of  $\mathcal{W}$ . However, since this projection is rarely used in training DNNs, we follow Gupta et al. [2018] and omit it in Algorithm 1. More importantly, this theoretical bound depends on the trace norm of gradients and the spectral norm of weights, showing that the algorithm can make use of the low-rank property of gradients.*

One can easily check that this convergence rate for convex nonsmooth problems is  $\mathcal{O}(1/\sqrt{T})$ , the same as SGD [Zinkevich, 2003] (see below) and AdaGrad [Duchi et al., 2011]. **Comparison with SGD.** The convergence rate for SGD under the assumptions of Corollary 2 is:

$$\text{SGD: } \frac{1}{T} \sum_{t=0}^{T-1} \mathbb{E}[f(W_t)] - f(W_*) \leq \mathcal{O} \left( \frac{D_F \|Q\|_F}{\sqrt{T}} \right),$$

where  $D_F$  and  $\|Q\|_F$  are the Frobenius norm upper bounds for the weights and gradients, respectively. By comparing this bound with Corollary 2, we have

- $\|Q\|_F \leq \|Q\|_* \leq \sqrt{r_G} \|Q\|_F$ , where  $r_G$  is the rank of  $Q$ . Thus when  $G_t$  are low-rank, or have very imbalanced singular values,  $\|Q\|_*$  can be close to  $\|Q\|_F$ ;
- $D_F/\sqrt{r_D} \leq D_{\text{op}} \leq D_F$ , where  $r_D = \max \text{rank of}(W_t - W_*)$ . Thus, when  $W_t - W_*$  are relatively high-rank or have lots of singular values of a similar scale,  $D_{\text{op}}$  can be much smaller than  $D_F$ .

Therefore, ASGO should work well when  $G_t$  are low-rank and  $W_t - W_*$  are relatively high-rank. **Intuitions on ASGO in practical tasks.** We argue that low-rank  $G_t$  and relatively high-rank  $W_t - W_*$  should be common in many practical tasks, revealing the potential of ASGO in applications. As we have discussed in Section 2, gradients are commonly low-rank in DNNs, as verified by Zhao et al. [2021], Yang et al. [2023], Cosson et al. [2023]. Meanwhile, given the huge success of LoRA [Hu et al., 2022] in fine-tuning foundation models, which naturally asserts a low-rank total update in  $W$ , there

may seem to be a conflict to assume that  $W_t - W_*$  has a high rank. However, it has been observed that  $W_0 - W_*$  should be relatively high-rank to obtain a better result, at least in pretraining and some complex fine-tuning tasks for large foundation models [Lialin et al., 2023, Jiang et al., 2024b, Huang et al., 2025]. Further exploration of the connection between the rank of weight updates and the performance of algorithms is an interesting topic for future research. **Comparison with Full-Matrix AdaGrad and Shampoo.** Shampoo [Gupta et al., 2018] and the full-matrix AdaGrad [Duchi et al., 2011] achieve the following convergence rates under the same settings as Theorem 1.

$$\begin{aligned} \text{Full-Matrix AdaGrad: } & \mathcal{O} \left( D_F \sum_{j=1}^m \sum_{i=1}^n \sqrt{\sum_{t=0}^{T-1} [G_t]_{i,j}^2} \right) \\ \text{Shampoo: } & \mathcal{O} \left( \sqrt{r} D_F \cdot \text{tr} \left( \left( \sum_{t=0}^{T-1} G_t G_t^\top \right)^{\frac{1}{4}} \right) \cdot \text{tr} \left( \left( \sum_{t=0}^{T-1} G_t^\top G_t \right)^{\frac{1}{4}} \right) \right). \end{aligned}$$

We can check that Theorem 1 indicates a convergence speed that is at least  $D_F/D_{\text{op}}$  times faster than full-matrix AdaGrad and  $\sqrt{r} D_F/D_{\text{op}}$  times faster than Shampoo; (see Appendix E for proofs). This also provides theoretical evidence that single-side preconditioning may be better at exploiting low-rankness of gradients, yielding a faster convergence speed compared to Shampoo-like preconditioning.

**Remark 2.** *Proofs of all of the results in this section are given in Appendix E. We keep the matrix structure of  $W_t$  and  $G_t$  throughout our analysis, in contrast to standard analyses of the convergence of AdaGrad and Shampoo, which are based on vectorizations of  $W_t$  and  $G_t$ . This is important for proving that ASGO can exploit the structured properties.*

## 5 Smooth Theory

It is also important to study the performance of Algorithm 1 in smooth settings, as many real training tasks have been widely observed to be smooth, at least locally. Also, only in smooth settings can we properly describe the importance of batch size.

**Assumption 2** (Smoothness).  *$f$  is 1-smooth with respect to  $\|\cdot\|_L$ , where  $L \in \mathbb{R}^{m \times m}$  is a symmetric positive definite matrix and for any  $X \in \mathbb{R}^{m \times n}$ ,*

$$\|X\|_L^2 \triangleq \text{tr}(X^\top L X).$$

If  $X = [x_1, \dots, x_n]$ , where each  $x_i \in \mathbb{R}^m$ , and we vectorize  $X$ , i.e.,  $\mathbf{x} \equiv \text{vec}(X) = (x_1^\top, \dots, x_n^\top)^\top$ , and form the block diagonal matrix  $\mathbf{L} \triangleq \text{diag}[L, \dots, L]$ , we obtain that  $\text{tr}(X^\top L X) = \sum_{i=1}^n x_i^\top L x_i = \mathbf{x}^\top \mathbf{L} \mathbf{x}$ . This means that Assumption 2 is equivalent to the existence of a symmetric matrix  $L \in \mathbb{R}^{m \times m}$ ,  $L \succ 0$  such that for any  $w \in \mathbb{R}^m$ ,  $-\mathbf{L} \preceq \nabla^2 f_v(\mathbf{w}) \preceq \mathbf{L}$ , where  $f_v(\mathbf{w}) = f(W)$ ,  $W = [w_1, \dots, w_n] \in \mathbb{R}^{m \times n}$  and  $\mathbf{w} \equiv \text{vec}(W) = [w_1^\top, \dots, w_n^\top]^\top \in \mathbb{R}^{mn}$ . Hence, it is closely related to the block-wise diagonal structure of the Hessian as observed by many researchers; (see Figure 3 in Appendix A). Also note that Assumption 2 implies the standard smoothness assumption with respect to the Frobenius norm by  $\|\nabla f_v(\mathbf{w})\|_{\text{op}} \leq \|L\|_{\text{op}}$ . This block-wise diagonal smoothness is an extension of the standard smoothness, which is related to but different from the diagonal anisotropic smoothness employed for analyzing sign-based and adaptive gradient methods [Bernstein et al., 2018, Liu et al., 2024].

**Assumption 3** (Variance). *Let  $N_t \triangleq \nabla f(W_t; \xi) - \nabla f(W_t) \in \mathbb{R}^{m \times n}$  be the stochastic gradient noise. We assume that  $\mathbb{E}[N_t] = 0$  and there exists a symmetric positive definite matrix  $V$  such that*

$$\mathbb{E}[N_t N_t^\top] \preceq V^2.$$

One can check that Assumption 3 implies the standard variance bound  $\mathbb{E}[\|N_t\|_F^2] \leq \|V\|_F^2$ . The assumption shares some similarity with the coordinate-wise variance bounds in Bernstein et al. [2018], Crawshaw et al. [2022], Liu et al. [2024], in the sense that it allows a more fine-grained analysis. This matrix-form variance upper bound may better describe the real case since it takes the structure of the noise into account, which is relevant to matrix rank and other structured properties.

**Theorem 3** (Smooth Convergence). *Under Assumptions 1, 2 and 3, for Algorithm 1 with  $\eta_t \equiv \eta = D_{\text{op}}$  and a batch size of  $M$ , it holds that*

$$\frac{1}{T} \sum_{t=0}^{T-1} \mathbb{E}[f(W_t)] - f(W_*) \leq \frac{4D_{\text{op}}^2 \|L\|_*}{T} + \frac{2\sqrt{2}D_{\text{op}} \|V\|_*}{\sqrt{MT}} + \frac{2\epsilon D_{\text{F}}^2}{D_{\text{op}} T},$$

where  $D_{\text{op}} \triangleq \max_{0 \leq t \leq T-1} \|W_t - W_*\|_{\text{op}}$ , and  $D_{\text{F}} \triangleq \max_{0 \leq t \leq T-1} \|W_t - W_*\|_{\text{F}}$ .

As discussed in Section 4,  $D_{\text{op}}$  and  $D_{\text{F}}$  can be bounded if we add a projection step in the update. The convergence rate specified in Theorem 3 is similar to the rate in Corollary 2 if the batch size  $M$  is small, when the  $\mathcal{O}(1/\sqrt{MT})$  term dominates the rate, and thus shares the same properties as we discussed in Section 4. This means that ASGO can benefit if the stochastic gradient noise  $V$  is generally low-rank. Furthermore, when the batch size  $M$  is large so that the  $\mathcal{O}(\|L\|_*/T)$  term contributes significantly to the bound, Theorem 3 implies more, which we now discuss.

**Comparison with SGD.** The convergence rate of SGD [Garrigos and Gower, 2023] is:

$$\text{SGD: } \frac{1}{T} \sum_{t=0}^{T-1} \mathbb{E}[f(W_t)] - f(W_*) \leq \mathcal{O} \left( \frac{D_{\text{F}}^2 \|L\|_{\text{op}}}{T} + \frac{D_{\text{F}} \|V\|_{\text{F}}}{\sqrt{MT}} \right),$$

where  $D_{\text{F}}$  is defined in Theorem 3. Since the comparison between the  $\mathcal{O}(1/\sqrt{MT})$  term is generally consistent with the discussion in Section 4, we further compare the  $\mathcal{O}(1/T)$  term here to provide some more intuition: we have

- $\|L\|_{\text{op}} \leq \|L\|_* \leq r_L \|L\|_{\text{op}}$ , where  $r_L$  is the rank of  $L$ . Thus when  $L$  is low-rank, or has very imbalanced singular values,  $\|L\|_*$  can be close to  $\|L\|_{\text{op}}$ ;
- $D_{\text{F}}/\sqrt{r_D} \leq D_{\text{op}} \leq D_{\text{F}}$ , where  $r_D = \max \text{rank of } (W_t - W_*)$ . Thus when  $W_t - W_*$  are of relatively high-rank or have lots of singular values of a similar scale,  $D_{\text{op}}$  can be much smaller than  $D_{\text{F}}$ .

Therefore, we can see that in general, ASGO should work well when the Hessian can be well approximated by a block-wise diagonal matrix with a low-rank  $L$  for each block and  $W_t - W_*$  are of relatively high-rank. Note that Hessians have been found to be low-rank in DNNs, especially after some steps of training [Sagun et al., 2016, 2017, Wu et al., 2020]. **Block-wise diagonal structure of DNNs.** It has been widely observed that the Hessian of MLPs and other DNNs, are approximately block-wise diagonal [Collobert, 2004, Zhang et al., 2024a,b, Bahamou et al., 2022], as shown in Figure 3 in Appendix A. This block-wise diagonal structure naturally arises from the structure of MLPs, where all the parameters associated with a particular neuron (i.e., all elements of either a row or column of  $W$ ) are more closely related and have a denser block Hessian matrix, than a set of parameters that do not share such an association. Intuitively, the elements of the rows of  $W$  seem to be more likely to be closely related to the columns of  $W$ . Based on Theorem 3, our algorithm should perform well in this block Hessian setting, showing great potential in real applications. **Intuition on single-side preconditioners.** Since ASGO only uses single-side preconditioners, it is important to determine on which side they should be applied. As demonstrated in Figure 3, a block in the Hessian commonly corresponds to all input weights into a neuron in the next layer, i.e., as a row of  $W$ . Therefore, we may want the single-side preconditioner to be on the right side of  $G_t$ . Based on this block-wise diagonal structure, Shampoo-like double-sided preconditioners may not only suffer from higher memory and computation costs, but also may precondition less effectively, since they are trying to approximate the structured curvature information matrix using a dense matrix produced by a Kronecker product [Gupta et al., 2018, Morwani et al., 2024].

**Remark 3.** *The proof of Theorem 3 is given in Appendix F. The analysis is similar in its general outline to the smooth analysis for AdaGrad [Levy et al., 2018, Liu et al., 2024], but it is more complex because of the involvement of matrix operations in ASGO.*

## 6 Further Discussions on ASGO

**Connection with Muon.** Muon [Jordan et al., 2024] can be interpreted as a standard steepest descent algorithm utilizing the spectral norm [Bernstein and Newhouse, 2024b] with momentum. If we

ignore the incorporated momentum, Muon computes

$$W_{t+1} = \operatorname{argmin}_{W \in \mathbb{R}^{m \times n}} \left\{ \langle G_t, W - W_t \rangle + \frac{1}{2\eta_t} \|W - W_t\|_{\text{op}}^2 \right\}, \quad (2)$$

preserving the matrix structure of the problem and naturally exploiting the structured properties because of the involvement of spectral norm in the steepest descent framework. This aligns with ASGO’s exploitation of structured properties. Moreover, if we ignore the momentum in both the gradient and the preconditioner, we can see that ASGO is equivalent to Muon.<sup>1</sup> Interestingly, this equivalence between ASGO and Muon in both theoretical basis and algorithm design is analogous to that between diagonal AdaGrad and SignSGD [Bernstein et al., 2018, Kunstner et al., 2023]. In this sense, we may interpret ASGO and Muon as AdaGrad and SignSGD for structured gradients, respectively. Note that Shampoo also admits such a relation with Muon in algorithmic design. However, as discussed in Section 4, Shampoo has a worse convergence rate and thus fails to benefit from the structured properties as does ASGO. To some extent, this means that ASGO may be a more appropriate approach than Shampoo as such an analog to diagonal AdaGrad.

From this intuition, we may also conjecture what the nonconvex convergence rate of ASGO is based on what it is for Muon. Hence, we prove in Appendix G that this rate for Muon is:

$$\min_{0 \leq t \leq T-1} \|\nabla f(W_t)\|_*^2 \leq \mathcal{O} \left( \frac{\|L\|_* (f(W_0) - f^*)}{T} \right), \quad (3)$$

where we assume that  $f^* \triangleq \inf f(W) > -\infty$ . Since diagonal AdaGrad and SignSGD have the same convergence rate in nonconvex settings up to logarithmic factors [Bernstein et al., 2018, Sun et al., 2023, Liu et al., 2024], we expect that ASGO has a nonconvex convergence rate comparable to (3) obtained by Muon up to logarithmic factors. It is an interesting future topic to prove this conjecture and further explore the nonconvex behavior of ASGO theoretically. Also, we note that as an intuitively smoother version of Muon, ASGO has good convergence properties in nonsmooth settings as shown in Section 4, where Muon, like SignSGD [Bernstein et al., 2018], may fail to converge [Karimireddy et al., 2019].

**Remark 4.** *However, in smooth settings, nonconvex convergence analysis of Muon has been presented in Li and Hong [2025]. They establish the convergence results under a more general setting, involving gradient noise and momentum following the analysis in Cutkosky and Mehta [2020]. However, if we only look at the deterministic case, their result is worse than (3) because of the explicit dependence on the dimension  $n$ . The key here is that the standard smoothness condition with respect to the Frobenius norm is not a good fit for analyzing structured gradient algorithms like Muon or ASGO. Using Assumption 2, we obtain better convergence results for Muon in (3).*

**Practical Implementations of ASGO.** We also provide Algorithm 2, a practical implementation of ASGO inspired by Adam [Kingma and Ba, 2014] and distributed Shampoo [Shi et al., 2023], together with a memory efficient diagonal variant of ASGO, named DASGO in Algorithm 3. DASGO is basically a light-weight optimizer with the preconditioner  $\Lambda_t$  of ASGO being diagonalized, which is efficient in both memory and computations. Please refer to Appendix B for details.

## 7 Empirical Results

We empirically evaluate the effectiveness of ASGO (Algorithm 2) and DASGO (Algorithm 3) on pretraining and finetuning tasks for Large Language (LL) models. We compare the methods against established optimizers, including AdamW [Kingma and Ba, 2014, Loshchilov and Hutter, 2017], Shampoo [Gupta et al., 2018], and Muon [Jordan et al., 2024]. Several important implementational details should be noted for fair comparison. First, since Muon is designed to operate exclusively on matrix parameters, we follow Jordan et al. [2024] and apply AdamW update rules to all 1D parameters within the Muon optimizer to ensure that it can handle the complete model. All experiments were conducted using NVIDIA V100s SMX2 GPUs. Specifically, for the larger-scale pretraining of GPT2, we utilized a configuration of four V100 GPUs, while other experiments were performed on a single V100 GPU.

<sup>1</sup>A proof of this equivalence can be found in Appendix G.

## 7.1 Pretraining NanoGPT

We first conducted experiments using the NanoGPT architecture on the Shakespeare character dataset, following the configuration in [Karpathy, 2022]. To ensure a fair comparison, we maintained consistent hyperparameter (HP) settings varying only those parameters that significantly impacted optimizer performance, i.e., learning rate, 1st and 2nd order moment coefficients ( $\beta_1$  and  $\beta_2$ ) and so on)<sup>2</sup>. For consistency across all optimization methods, we employ the OneCycleLR learning rate schedule, which has been shown to provide stable convergence properties in deep learning tasks. Figure 1 presents a comparison of the pretraining performance of ASGO and DASGO with that of Shampoo, Muon and AdamW on the NanoGPT model. See Appendix C for a plot of the training loss. Examining both test and training loss curves, ASGO consistently outperforms Shampoo despite requiring only half the memory consumption and computational effort, which highlights ASGO’s practical advantages for training language models. Furthermore, ASGO and Muon achieve the lowest final training and test losses, outperforming all other methods. This consistent performance between ASGO and Muon aligns well with our discussions in Section 6. Moreover, The lightweight DASGO optimizer achieves competitive results against AdamW in both training and test loss metrics. DASGO demonstrates particularly strong performance during the initial training phase (first 200 training steps, which is about the first two epochs), but eventually exhibits a performance gap with ASGO. We will discuss this performance gap in Section 7.2.

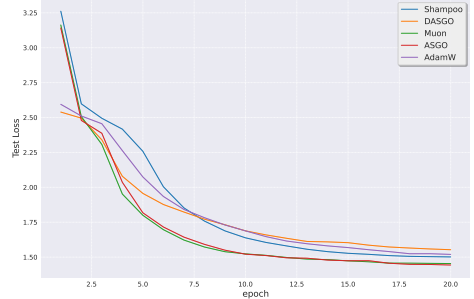


Figure 1: Validation Loss for NanoGPT

## 7.2 Pretraining GPT2

To further evaluate the efficacy of ASGO and DASGO, we extended our investigation to larger-scale pretraining tasks. We adopted the configuration of the GPT2 model as described by [Karpathy, 2022]. In this setting, the GPT2 model comprises 12 Transformer blocks, each with a hidden dimension of 768. Consequently, there are 12 projection layers with dimensions  $768 \times 2304$ . In each of these layers alone, Shampoo necessitates storing two matrices of size  $768 \times 768$  and two matrices of size  $2304 \times 2304$  for its state. In contrast, ASGO requires storing only two  $768 \times 768$  matrices, corresponding to the preconditioning and inverse preconditioning factors. This substantial difference in memory requirements rendered Shampoo impractical for our large-scale GPT2 pretraining experiments, preventing us from obtaining meaningful results within our computational constraints. Therefore, we do not report Shampoo’s performance in this setting. To ensure a fair comparison, we carefully tuned the learning rates and  $\beta_2$  values (where applicable) for all optimizers (tuning details are provided in Section C). Furthermore, we employed a learning rate schedule consisting of 200 linear warm-up steps followed by a cosine decay, which is a common practice for training LLM models. Figure 2a and Table 1 present a comparison of the training and validation loss achieved by ASGO and DASGO against Muon and AdamW on the GPT2 model. The training loss curves reveal that ASGO achieves a lower final training loss compared to AdamW in the pretraining task, suggesting superior optimization. This observation is further corroborated by the validation loss (Table 1), where ASGO’s performance (3.87) is better than AdamW’s (3.96). Interestingly, ASGO’s performance appears more similar to Muon (3.82) in terms of final loss, although ASGO exhibits a slightly higher validation loss than Muon.

Table 1: Pretraining GPT2 Validation Loss

AdamW	Muon	ASGO	DASGO
3.96	3.82	3.87	5.23

ASGO demonstrates potential advantages over Muon. As depicted in Figure 2a, ASGO shows a faster initial decrease in training loss. Furthermore, our learning rate sensitivity analysis (Figure 2b), with tested candidates  $[10^{-3}, 5 \times 10^{-3}, 10^{-2}, 3 \times 10^{-2}, 5 \times 10^{-2}, 7 \times 10^{-2}, 10^{-1}, 5 \times 10^{-1}]$  using optimal settings for Muon and ASGO suggests that ASGO might be more robust to learning rate selection. Specifically, at higher learning rates (e.g.,  $10^{-1}, 5 \times 10^{-1}$ ), ASGO maintains relatively stable training while Muon exhibits instability. These observations – faster initial convergence and a potentially wider stable learning rate regime for ASGO – are consistent with characteristics often associated with

<sup>2</sup>A full description of how these “best” HPs were selected and their values are presented in Appendix C.

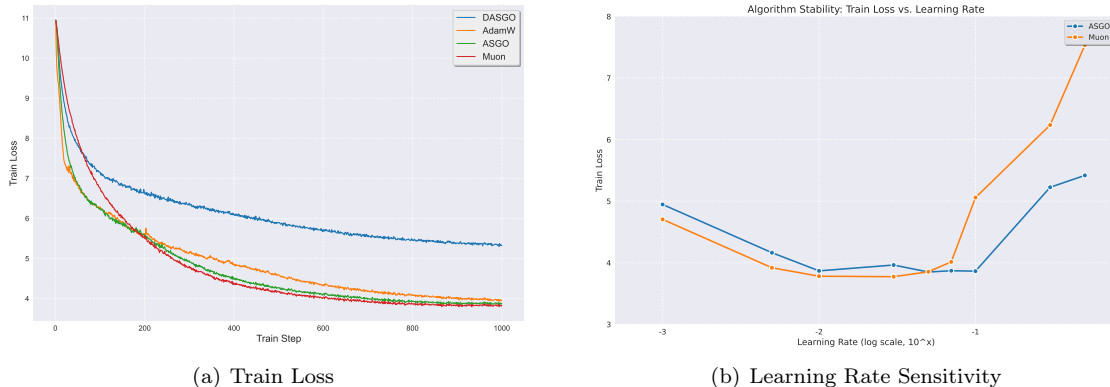


Figure 2: Pretraining Performance and Learning Rate Sensitivity on GPT2

adaptive optimization methods, as discussed in Section 6. However, DASGO (5.23) underperformed compared to AdamW, Muon, and ASGO in the GPT2 pretraining task. This performance gap was also observed in the pretraining of the smaller NanoGPT model. A primary reason for the difference between DASGO and ASGO likely stems from its diagonal preconditioning. By only retaining and using only the diagonal elements of the  $GG^T$ , DASGO essentially disregards the inter-dependencies between different parameter gradients from neurons within a layer, moving away from a true matrix-based adaptive approach towards a per-parameter scaling akin to vector-based methods. This highlights the value of preserving non-diagonal elements in the preconditioner matrices, particularly for capturing parameter interactions in attention-based architectures. Nevertheless, DASGO’s significantly reduced memory footprint makes it a compelling option for resource-limited settings where computational efficiency is paramount.

### 7.3 Finetuning GPT2-Large on WikiText-2

To further assess the performance of our proposed optimizers, we conducted fine-tuning experiments on the GPT2-Large(774M) model [Radford et al., 2019] using the WikiText-2 dataset. We explored two distinct fine-tuning objectives:

- First, we fine-tuned GPT2-Large using the standard Causal Language Modeling (CLM) loss, which is the conventional approach for autoregressive language models.
- Second, we also fine-tuned the same GPT2-Large model on WikiText-2 but employed the Fill-in-the-Middle (FIM) training objective, following the setting in [Bavarian et al., 2022]. The FIM objective modifies the training process to enable the model to learn to infill text by rearranging document spans.

To account for statistical variability, we conducted five experimental runs with different random seeds under the same hyperparameter settings. Table 2 presents the average perplexity results after fine-tuning for 2 epochs. For both objectives, we employed a cosine decay learning rate scheduler. Hyperparameter search details and 95% confidence intervals are provided in Table 6. Under the CLM objective, ASGO (13.88 perplexity) and DASGO (13.84 perplexity) achieved lower perplexity than both Muon (13.91 perplexity) and AdamW (14.01 perplexity). This suggests that both ASGO and its memory-efficient variant, DASGO, can be effective for traditional LL modeling fine-tuning. When the model was fine-tuned using the FIM objective, we observed a similar trend, with ASGO (15.66 perplexity) and DASGO (15.45 perplexity) outperforming both Muon (15.93 perplexity) and AdamW (17.46 perplexity). Across both fine-tuning scenarios, ASGO and DASGO demonstrated competitive or superior performance compared to these baseline optimizers.

Table 2: Finetuning GPT2-Large Perplexity

	AdamW	Muon	ASGO	DASGO
CLM	14.01	13.91	13.88	13.84
FIM	17.46	15.93	15.66	15.45

## 8 Conclusions

In this paper, we proposed a novel algorithm ASGO, which achieves significantly better convergence rates compared to full-matrix AdaGrad and Shampoo. Based on the theory, we demonstrated that

ASGO can benefit from low-rank gradients and block-wise diagonal Hessians, which are widely observed structured properties of DNNs. We further proposed some practical modifications to ASGO, and verified its effectiveness empirically. Currently, ASGO still has two major limitations: 1) computationally intensive compared to Adam because of the matrix operation; 2) it is not straightforward to extend the algorithm to apply to tensors. We plan to look into these issues in future work.

## References

- Tsuyoshi Ando, Chi-Kwong Li, and Roy Mathias. Geometric means. *Linear algebra and its applications*, 385:305–334, 2004.
- Achraf Bahamou, Donald Goldfarb, and Yi Ren. A mini-block fisher method for deep neural networks, 2022. URL <https://arxiv.org/abs/2202.04124>.
- Mohammad Bavarian, Heewoo Jun, Nikolas Tezak, John Schulman, Christine McLeavey, Jerry Tworek, and Mark Chen. Efficient training of language models to fill in the middle, 2022. URL <https://arxiv.org/abs/2207.14255>.
- James Bergstra and Yoshua Bengio. Random search for hyper-parameter optimization. *Journal of Machine Learning Research*, 13(10):281–305, 2012. URL <http://jmlr.org/papers/v13/bergstra12a.html>.
- Jeremy Bernstein and Laker Newhouse. Modular duality in deep learning. *arXiv preprint arXiv:2410.21265*, 2024a.
- Jeremy Bernstein and Laker Newhouse. Old optimizer, new norm: An anthology. *arXiv preprint arXiv:2409.20325*, 2024b.
- Jeremy Bernstein, Yu-Xiang Wang, Kamyar Azizzadenesheli, and Animashree Anandkumar. signsgd: Compressed optimisation for non-convex problems. In *International Conference on Machine Learning*, pages 560–569. PMLR, 2018.
- Tom Brown, Benjamin Mann, Nick Ryder, Melanie Subbiah, Jared D Kaplan, Prafulla Dhariwal, Arvind Neelakantan, Pranav Shyam, Girish Sastry, Amanda Askell, Sandhini Agarwal, Ariel Herbert-Voss, Gretchen Krueger, Tom Henighan, Rewon Child, Aditya Ramesh, Daniel Ziegler, Jeffrey Wu, Clemens Winter, Chris Hesse, Mark Chen, Eric Sigler, Mateusz Litwin, Scott Gray, Benjamin Chess, Jack Clark, Christopher Berner, Sam McCandlish, Alec Radford, Ilya Sutskever, and Dario Amodei. Language models are few-shot learners. In H. Larochelle, M. Ranzato, R. Hadsell, M.F. Balcan, and H. Lin, editors, *Advances in Neural Information Processing Systems*, volume 33, pages 1877–1901. Curran Associates, Inc., 2020. URL <https://proceedings.neurips.cc/paper/2020/file/1457c0d6bfc4967418bfb8ac142f64a-Paper.pdf>.
- Dami Choi, Christopher J Shallue, Zachary Nado, Jaehoon Lee, Chris J Maddison, and George E Dahl. On empirical comparisons of optimizers for deep learning. *arXiv preprint arXiv:1910.05446*, 2019.
- Ronan Collobert. Large scale machine learning. 2004.
- Romain Cosson, Ali Jadbabaie, Anuran Makur, Amirhossein Reisizadeh, and Devavrat Shah. Low-rank gradient descent. *IEEE Open Journal of Control Systems*, 2:380–395, 2023.
- Michael Crawshaw, Mingrui Liu, Francesco Orabona, Wei Zhang, and Zhenxun Zhuang. Robustness to unbounded smoothness of generalized signsgd. *Advances in neural information processing systems*, 35:9955–9968, 2022.
- Ashok Cutkosky and Harsh Mehta. Momentum improves normalized sgd. In *International conference on machine learning*, pages 2260–2268. PMLR, 2020.
- Jacob Devlin, Ming-Wei Chang, Kenton Lee, and Kristina Toutanova. Bert: Pre-training of deep bidirectional transformers for language understanding. *arXiv preprint arXiv:1810.04805*, 2018.
- John Duchi, Elad Hazan, and Yoram Singer. Adaptive subgradient methods for online learning and stochastic optimization. *Journal of machine learning research*, 12(7), 2011.
- Vladimir Feinberg, Xinyi Chen, Y Jennifer Sun, Rohan Anil, and Elad Hazan. Sketchy: Memory-efficient adaptive regularization with frequent directions. *Advances in Neural Information Processing Systems*, 36:75911–75924, 2023.
- Guillaume Garrigos and Robert M Gower. Handbook of convergence theorems for (stochastic) gradient methods. *arXiv preprint arXiv:2301.11235*, 2023.

- Vineet Gupta, Tomer Koren, and Yoram Singer. A unified approach to adaptive regularization in online and stochastic optimization. *arXiv preprint arXiv:1706.06569*, 2017.
- Vineet Gupta, Tomer Koren, and Yoram Singer. Shampoo: Preconditioned stochastic tensor optimization. In *International Conference on Machine Learning*, pages 1842–1850. PMLR, 2018.
- Guy Gur-Ari, Daniel A Roberts, and Ethan Dyer. Gradient descent happens in a tiny subspace. *arXiv preprint arXiv:1812.04754*, 2018.
- Nicholas J. Higham. *Functions of Matrices: Theory and Computation*. Society for Industrial and Applied Mathematics, United States, 2008. ISBN 9780898717778. ISBN 978-0-898716-46-7.
- Edward J Hu, Yelong Shen, Phillip Wallis, Zeyuan Allen-Zhu, Yuanzhi Li, Shean Wang, Lu Wang, Weizhu Chen, et al. Lora: Low-rank adaptation of large language models. *ICLR*, 1(2):3, 2022.
- Qiushi Huang, Tom Ko, Zhan Zhuang, Lilian Tang, and Yu Zhang. Hira: Parameter-efficient hadamard high-rank adaptation for large language models. In *The Thirteenth International Conference on Learning Representations*, 2025.
- Ruichen Jiang, Devyani Maladkar, and Aryan Mokhtari. Convergence analysis of adaptive gradient methods under refined smoothness and noise assumptions. *arXiv preprint arXiv:2406.04592*, 2024a.
- Ting Jiang, Shaohan Huang, Shengyue Luo, Zihan Zhang, Haizhen Huang, Furu Wei, Weiwei Deng, Feng Sun, Qi Zhang, Deqing Wang, et al. Mora: High-rank updating for parameter-efficient fine-tuning. *arXiv preprint arXiv:2405.12130*, 2024b.
- Keller Jordan, Yuchen Jin, Vlado Boza, You Jiacheng, Franz Cesista, Laker Newhouse, and Jeremy Bernstein. Muon: An optimizer for hidden layers in neural networks, 2024. URL <https://kellerjordan.github.io/posts/muon/>.
- Sai Praneeth Karimireddy, Quentin Rebjock, Sebastian Stich, and Martin Jaggi. Error feedback fixes signsgd and other gradient compression schemes. In *International Conference on Machine Learning*, pages 3252–3261. PMLR, 2019.
- Andrej Karpathy. NanoGPT. <https://github.com/karpathy/nanoGPT>, 2022.
- Diederik P Kingma and Jimmy Ba. Adam: A method for stochastic optimization. *arXiv preprint arXiv:1412.6980*, 2014.
- Frederik Kunstner, Jacques Chen, Jonathan Wilder Lavington, and Mark Schmidt. Noise is not the main factor behind the gap between sgd and adam on transformers, but sign descent might be. *arXiv preprint arXiv:2304.13960*, 2023.
- Tim Large, Yang Liu, Minyoung Huh, Hyojin Bahng, Phillip Isola, and Jeremy Bernstein. Scalable optimization in the modular norm. *arXiv preprint arXiv:2405.14813*, 2024.
- Kfir Y Levy, Alp Yurtsever, and Volkan Cevher. Online adaptive methods, universality and acceleration. *Advances in neural information processing systems*, 31, 2018.
- Jiaxiang Li and Mingyi Hong. A note on the convergence of muon and further. *arXiv preprint arXiv:2502.02900*, 2025.
- Vladislav Lialin, Namrata Shivagunde, Sherin Muckatira, and Anna Rumshisky. Relora: High-rank training through low-rank updates. *arXiv preprint arXiv:2307.05695*, 2023.
- Wu Lin, Felix Dangel, Runa Eschenhagen, Juhan Bae, Richard E. Turner, and Alireza Makhzani. Can we remove the square-root in adaptive gradient methods? a second-order perspective, 2024. URL <https://arxiv.org/abs/2402.03496>.
- Jingyuan Liu, Jianlin Su, Xingcheng Yao, Zhejun Jiang, Guokun Lai, Yulun Du, Yidao Qin, Weixin Xu, Enzhe Lu, Junjie Yan, et al. Muon is scalable for llm training. *arXiv preprint arXiv:2502.16982*, 2025a.

- Liming Liu, Zhenghao Xu, Zixuan Zhang, Hao Kang, Zichong Li, Chen Liang, Weizhu Chen, and Tuo Zhao. Cosmos: A hybrid adaptive optimizer for memory-efficient training of llms. *arXiv preprint arXiv:2502.17410*, 2025b.
- Yuxing Liu, Rui Pan, and Tong Zhang. Adagrad under anisotropic smoothness. *arXiv preprint arXiv:2406.15244*, 2024.
- Ilya Loshchilov and Frank Hutter. Decoupled weight decay regularization. *arXiv preprint arXiv:1711.05101*, 2017.
- Karl Löwner. Über monotone matrixfunktionen. *Mathematische Zeitschrift*, 38(1):177–216, 1934.
- James Martens and Roger Grosse. Optimizing neural networks with kronecker-factored approximate curvature. In *International conference on machine learning*, pages 2408–2417. PMLR, 2015.
- Depen Morwani, Itai Shapira, Nikhil Vyas, Eran Malach, Sham Kakade, and Lucas Janson. A new perspective on shampoo’s preconditioner. *arXiv preprint arXiv:2406.17748*, 2024.
- Yurii Nesterov et al. *Lectures on convex optimization*, volume 137. Springer, 2018.
- Son Nguyen, Bo Liu, Lizhang Chen, and Qiang Liu. Improving adaptive moment optimization via preconditioner diagonalization. *arXiv preprint arXiv:2502.07488*, 2025.
- Long Ouyang, Jeffrey Wu, Xu Jiang, Diogo Almeida, Carroll Wainwright, Pamela Mishkin, Chong Zhang, Sandhini Agarwal, Katarina Slama, Alex Ray, et al. Training language models to follow instructions with human feedback. *Advances in Neural Information Processing Systems*, 35:27730–27744, 2022.
- Alec Radford, Jeffrey Wu, Rewon Child, David Luan, Dario Amodei, Ilya Sutskever, et al. Language models are unsupervised multitask learners. *OpenAI blog*, 1(8):9, 2019.
- Yi Ren and Donald Goldfarb. Tensor normal training for deep learning models, 2021. URL <https://arxiv.org/abs/2106.02925>.
- Levent Sagun, Leon Bottou, and Yann LeCun. Eigenvalues of the hessian in deep learning: Singularity and beyond. *arXiv preprint arXiv:1611.07476*, 2016.
- Levent Sagun, Utku Evci, V Ugur Guney, Yann Dauphin, and Leon Bottou. Empirical analysis of the hessian of over-parametrized neural networks. *arXiv preprint arXiv:1706.04454*, 2017.
- Noam Shazeer and Mitchell Stern. Adafactor: Adaptive learning rates with sublinear memory cost. In *International Conference on Machine Learning*, pages 4596–4604. PMLR, 2018.
- Hao-Jun Michael Shi, Tsung-Hsien Lee, Shintaro Iwasaki, Jose Gallego-Posada, Zhijing Li, Kaushik Rangadurai, Dheevatsa Mudigere, and Michael Rabbat. A distributed data-parallel pytorch implementation of the distributed shampoo optimizer for training neural networks at-scale. *arXiv preprint arXiv:2309.06497*, 2023.
- Matthew Streeter and H Brendan McMahan. Less regret via online conditioning. *arXiv preprint arXiv:1002.4862*, 2010.
- Tao Sun, Qingsong Wang, Dongsheng Li, and Bao Wang. Momentum ensures convergence of signsgd under weaker assumptions. In *International Conference on Machine Learning*, pages 33077–33099. PMLR, 2023.
- Hugo Touvron, Louis Martin, and Kevin Stone. Llama 2: Open Foundation and Fine-Tuned Chat Models.
- Hugo Touvron, Thibaut Lavril, Gautier Izacard, Xavier Martinet, Marie-Anne Lachaux, Timothée Lacroix, Baptiste Rozière, Naman Goyal, Eric Hambro, Faisal Azhar, Aurelien Rodriguez, Armand Joulin, Edouard Grave, and Guillaume Lample. LLaMA: Open and Efficient Foundation Language Models. 2023. doi: 10.48550/ARXIV.2302.13971. URL <https://arxiv.org/abs/2302.13971>. Publisher: arXiv Version Number: 1.

- Nikhil Vyas, Depen Morwani, Rosie Zhao, Itai Shapira, David Brandfonbrener, Lucas Janson, and Sham Kakade. Soap: Improving and stabilizing shampoo using adam. *arXiv preprint arXiv:2409.11321*, 2024.
- Hongyi Wang, Scott Sievert, Shengchao Liu, Zachary Charles, Dimitris Papailiopoulos, and Stephen Wright. Atomo: Communication-efficient learning via atomic sparsification. *Advances in neural information processing systems*, 31, 2018.
- Rachel Ward, Xiaoxia Wu, and Leon Bottou. Adagrad stepsizes: Sharp convergence over nonconvex landscapes. *The Journal of Machine Learning Research*, 21(1):9047–9076, 2020.
- Yikai Wu, Xingyu Zhu, Chenwei Wu, Annie Wang, and Rong Ge. Dissecting hessian: Understanding common structure of hessian in neural networks. *arXiv preprint arXiv:2010.04261*, 2020.
- Shuo Xie, Mohamad Amin Mohamadi, and Zhiyuan Li. Adam exploits  $\ell_\infty$ -geometry of loss landscape via coordinate-wise adaptivity. *arXiv preprint arXiv:2410.08198*, 2024.
- Shuo Xie, Tianhao Wang, Sashank Reddi, Sanjiv Kumar, and Zhiyuan Li. Structured preconditioners in adaptive optimization: A unified analysis. *arXiv preprint arXiv:2503.10537*, 2025.
- Yuege Xie, Xiaoxia Wu, and Rachel Ward. Linear convergence of adaptive stochastic gradient descent. In *International conference on artificial intelligence and statistics*, pages 1475–1485. PMLR, 2020.
- Greg Yang, James B Simon, and Jeremy Bernstein. A spectral condition for feature learning. *arXiv preprint arXiv:2310.17813*, 2023.
- Yang You, Jing Li, Sashank Reddi, Jonathan Hseu, Sanjiv Kumar, Srinadh Bhojanapalli, Xiaodan Song, James Demmel, Kurt Keutzer, and Cho-Jui Hsieh. Large batch optimization for deep learning: Training bert in 76 minutes. *arXiv preprint arXiv:1904.00962*, 2019.
- Yushun Zhang, Congliang Chen, Tian Ding, Ziniu Li, Ruoyu Sun, and Zhi-Quan Luo. Why transformers need adam: A hessian perspective. *arXiv preprint arXiv:2402.16788*, 2024a.
- Yushun Zhang, Congliang Chen, Ziniu Li, Tian Ding, Chenwei Wu, Diederik P Kingma, Yinyu Ye, Zhi-Quan Luo, and Ruoyu Sun. Adam-mini: Use fewer learning rates to gain more. *arXiv preprint arXiv:2406.16793*, 2024b.
- Jiawei Zhao, Florian Schäfer, and Anima Anandkumar. Zero initialization: Initializing neural networks with only zeros and ones. *arXiv preprint arXiv:2110.12661*, 2021.
- Jiawei Zhao, Zhenyu Zhang, Beidi Chen, Zhangyang Wang, Anima Anandkumar, and Yuandong Tian. Galore: Memory-efficient llm training by gradient low-rank projection. *arXiv preprint arXiv:2403.03507*, 2024.
- Martin Zinkevich. Online convex programming and generalized infinitesimal gradient ascent. In *Proceedings of the 20th international conference on machine learning (icml-03)*, pages 928–936, 2003.

## A Additional Related Work

**Optimization with Matrix Structure.** Much recent work has focused on improving full-matrix AdaGrad and Shampoo. Feinberg et al. [2023] uses a sketching-based approach to approximate the full-matrix AdaGrad preconditioner with lower memory cost. Morwani et al. [2024] provides theoretical intuition and empirical evidence to claim that Shampoo should use the  $-1/2$  power in its preconditioners to better approximate the Empirical Fisher (EF) matrix. Vyas et al. [2024] demonstrates that Shampoo is like doing Adafactor in the eigenspace of gradients and proposes a novel algorithm, SOAP, that performs Adam in this eigenspace. SOAP is observed to achieve better performance than Adam and Shampoo, but suffers from a high computation load per iteration. Galore [Zhao et al., 2024] shares a similar algorithmic design with SOAP with extra focus on lowering memory costs. Muon [Jordan et al., 2024] follows this line of work, using a steepest descent (in the spectral norm) framework, which it shows to be scalable and effective in training large foundation models [Liu et al., 2025a]. Large et al. [2024], Bernstein and Newhouse [2024a] propose the modular approach that has also been applied to improve Muon. More recently, Nguyen et al. [2025] proposes AdaDiag, which may be viewed as SOAP doing SVD without gradient accumulation. Liu et al. [2025b] proposes COSMOS, a combination of SOAP and Muon, that trades off between performance and computational efficiency.

**Rank of Gradients and Weight Updates.** It has been widely observed that gradients are naturally low-rank in DNNs, even when a large batch size is employed [Gur-Ari et al., 2018, Zhao et al., 2021, Yang et al., 2023, Cosson et al., 2023]. This property has been widely utilized for computation and memory efficiency in training [Wang et al., 2018, Cosson et al., 2023, Zhao et al., 2024]. On the other hand, the rank of the total weight update  $\Delta W = W_T - W_0$ , depends a lot on the training method. If we use LoRA [Hu et al., 2022],  $\Delta W$  is determined to be low-rank. However, in pretraining or even many complex fine-tuning tasks, LoRA’s performance is much worse than methods that produce high-rank weight updates like full-parameter training, which is conjectured to be due to the weight update rank [Lialin et al., 2023, Jiang et al., 2024b, Huang et al., 2025].

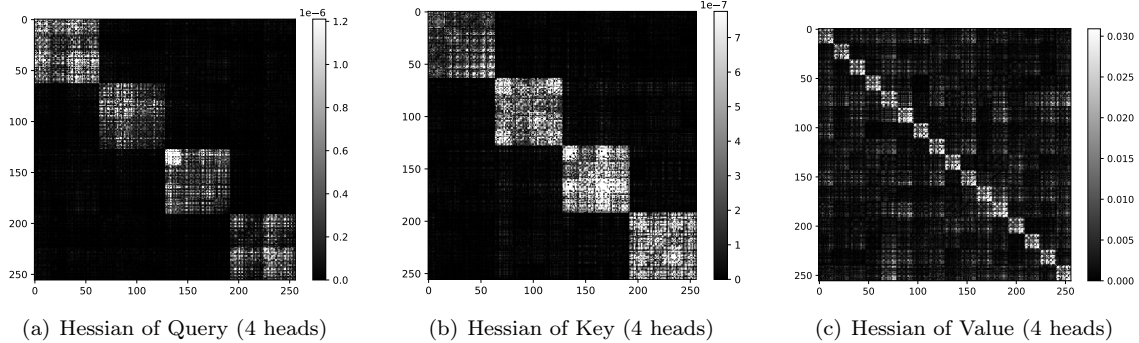


Figure 3: This figure is from Zhang et al. [2024b]. It depicts the Hessian of different parameter blocks in a small Transformer at the 1% training step. The near-block-diagonal structure maintains throughout training. But different parameter blocks have different numbers of small dense matrices, where Query and Key correspond to the number of heads.

**Block-wise Diagonal Hessian.** It has been observed that the Hessian of a neural network tends to be block-wise diagonal with each block corresponding to a neuron both in experiments and theory for small MLPs [Collobert, 2004]. Zhang et al. [2024a,b] recently numerically verified this property in small transformers, and as illustrated in Figure 4, further empirically showed that transformers may exhibit heterogeneity between blocks, while CNNs may not.

**Concurrent Work.** When we were finishing writing this paper, we noticed that the paper [Xie et al., 2025], which had just appeared on arXiv, proposes and studies an algorithm, referred to as One-Sided Shampoo, that is identical to ASGO. Although the theoretical techniques and convergence results proved in [Xie et al., 2025] and here are very similar in general, there are still some notable differences between the two works. First, the motivations are different. In Xie et al. [2025], the authors develop their method from the unified preconditioning method framework AdaptReg [Gupta et al.,

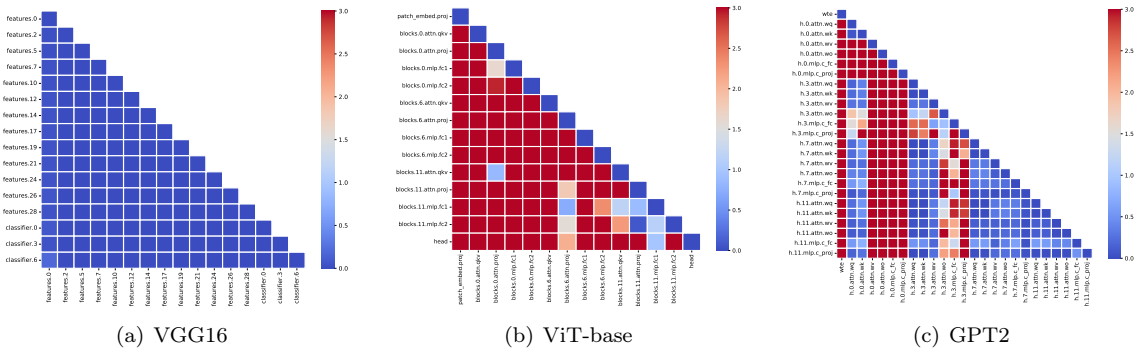


Figure 4: This figure is from Zhang et al. [2024a,b], calculating the Jensen-Shannon (JS) distance between two eigenvalue densities of all possible block pairs at initialization. It shows that JS distance of blockwise spectra in CNNs is significantly smaller than that in Transformers.

2017] and mainly highlight its superior convergence results compared to Shampoo and full-matrix AdaGrad. In our paper, we focus more on theoretically discussing how ASGO can utilize the structured properties of optimization problems including low-rank gradients and block-wise diagonal Hessians, to highlight the potential of ASGO as a practical algorithm for training deep learning models. Second, our empirical results provide evidence that ASGO can perform well in practical tasks, whereas Xie et al. [2025] focuses on convex settings and examines One-Sided Shampoo only on linear regression. Moreover, our implementation includes specialized designs for Transformer architectures (particularly query/key) to improve performance on deep learning training tasks. As a direct byproduct of our main algorithm, we also developed a lightweight diagonal version named DASGO to trade off memory consumption and performance. Third, Xie et al. [2025] focuses primarily on developing a general proof framework applicable to multiple optimizers including One-Sided Shampoo, whereas our work specifically examines the theoretical and practical benefits of ASGO. To conclude, both works contribute to a better understanding of ASGO/One-Sided Shampoo.

## B More Discussions on ASGO

**A practical implementation of ASGO.** We present a practical implementation of ASGO in Algorithm 2. Our implementation incorporates several common modifications to enhance computational efficiency and stability.

(i) A key modification is the adaptive selection of the preconditioning side. Instead of fixing the preconditioner to one side, we dynamically choose to precondition on the side corresponding to the smaller dimension of the gradient matrix  $G_t$  in  $\mathbb{R}^{D_1 \times D_2}$ . Specifically, if  $D_1 < D_2$ , the preconditioner is formed from  $G_t G_t^T$  and applied from the left; otherwise (if  $D_2 < D_1$ ), it is formed from  $G_t^T G_t$  and applied from the right. This strategy, which aims to minimize computational overhead associated with the preconditioner, is also used by the Muon Optimizer. For 1D parameters (i.e., gradient vectors  $g$ ), where one dimension is 1, this "smaller dimension" rule naturally leads to a scalar preconditioner (derived from  $g^T g$ ). This effectively implements a form of AdaGrad-Norm [Streeter and McMahan, 2010, Ward et al., 2020] for these vector parameters. Consequently, this unified approach allows ASGO to efficiently handle all parameter structures, including 1D vectors, without needing a separate optimizer (like AdamW [Loshchilov and Hutter, 2017]) that is often employed for such parameters in methods like Muon [Jordan et al., 2024]. The convergence guarantees can be extended to this adaptive side selection, as each choice (left or right preconditioning) maintains a valid ASGO-like update structure (operating on  $W$  or  $W^T$ , respectively)<sup>3</sup>.

(ii) Exponential moving averages are used to update the preconditioner and incorporate momentum, following established practice, which results in Adam’s improvements across various tasks over AdaGrad.

(iii) The preconditioner matrix is inverted every  $\tau$  iterations, as is done in distributed Shampoo [Shi et al., 2023] and SOAP [Vyas et al., 2024]. This modification increases memory requirements but substantially reduces computational overhead while improving algorithmic stability.

<sup>3</sup>For instance, applying ASGO with right-side preconditioning to  $W$  is equivalent to applying the original left-side ASGO formulation to  $W^T$ .

---

**Algorithm 2** A Practical Implementation of ASGO

---

```
1: Input:  $W_0 \in \mathbb{R}^{m \times n}$ , lr schedule  $\{\eta_t\}$ , momentums  $\beta_1, \beta_2 \in [0, 1)$ , batch size  $M \in \mathbb{N}$ , update  
   interval  $\tau \in \mathbb{N}$ ,  $\epsilon \in \mathbb{R}$  ( $\epsilon$  should be small, similar to the  $\epsilon$  for Adam or AdaGrad.)  
2: Initialize  $M_{-1} = 0 \in \mathbb{R}^{m \times n}$ ,  $V_{-1} = 0 \in \mathbb{R}^{n \times n}$  or  $\mathbb{R}^{m \times m}$   
3: for  $t = 0$  to  $T - 1$  do  
4:   Sample mini-batch  $\mathcal{B}_t$  with  $|\mathcal{B}_t| \equiv M$  uniformly  
5:    $G_t = \frac{1}{M} \sum_{\xi \in \mathcal{B}_t} \nabla_W f(W_t; \xi)$   
6:    $M_t = \beta_1 M_{t-1} + (1 - \beta_1) G_t$   
7:   if  $m < n$  then  
8:      $V_t = \beta_2 V_{t-1} + (1 - \beta_2) G_t G_t^\top$   
9:   else  
10:     $V_t = \beta_2 V_{t-1} + (1 - \beta_2) G_t^\top G_t$   
11:   end if  
12:   if  $\text{mod}(t, \tau) = 0$   
13:      $\Lambda_t^{\text{inv}} = (V_t + \epsilon I_n)^{-\frac{1}{2}}$   
14:   else  
15:      $\Lambda_t^{\text{inv}} = \Lambda_{t-1}^{\text{inv}}$   
16:   end if  
17:   if  $m < n$  then  
18:      $W_{t+1} = W_t - \eta_t \Lambda_t^{\text{inv}} M_t$   
19:   else  
20:      $W_{t+1} = W_t - \eta_t M_t \Lambda_t^{\text{inv}}$   
21:   end if  
22: end for
```

---

**Special Design for Transformers.** Furthermore, we introduce a specialized adaptation of ASGO for query and key matrices in attention layers. Recent work by Zhang et al. [2024b] has demonstrated that the Hessian structure of query and key layers differs significantly from conventional MLP layers. As illustrated in Figure 3, the number of dense blocks corresponds to the number of attention heads rather than output neurons. This observation aligns with the forward computation of multi-head attention, where attention scores are computed independently across different subspaces, suggesting that query and key parameters could be optimized in a head-wise manner. To leverage this insight, we reshape query and key parameters from matrices in  $\mathbb{R}^{n \times hd}$  to three-dimensional tensors  $\mathbb{R}^{h \times n \times d}$ , and apply our optimization algorithm independently to each head’s subspace. This restructuring reduces both memory consumption and computational complexity by decreasing the matrix size from  $O(h^2 d^2)$  into  $O(hd^2)$ . For instance, in NanoGPT [Karpathy, 2022], this adjustment reduces the preconditioning size of a single query/key parameter from approximately  $10^6$  elements into  $10^5$ . The empirical performance of this modification is evaluated in Section C.

**A Diagonal Variant of ASGO.** Drawing inspiration from Duchi et al. [2011], we also implement a variant of ASGO using diagonal matrices, which we denote as DASGO, presented in Algorithm 3. DASGO can be viewed as a lightweight version of ASGO, which eliminates the need to compute the inverse square root of full matrices, and reduces memory requirements to a level comparable with Adam-mini [Zhang et al., 2024b]. It also makes the choice of which side of  $M_t$  to precondition unimportant in terms of computational effort, in contrast to ASGO. For DASGO, we choose to apply the diagonal preconditioner on the right side, aligning with the neuron architecture in DNNs. However, since DASGO only employs a diagonal preconditioner, it fails to recover the superior theoretical properties of ASGO under block-wise diagonal Hessian settings. We further empirically examine this tradeoff in Section 7.

## C Details of Empirical Experiments

### C.1 Pretraining NanoGPT

**Experimental Setup:** As an initial experiment, we compared the performance of ASGO, DASGO, Muon, Shampoo, and Adam-W for training NanoGPT, which consists of 6 Transformer layers, 6

---

**Algorithm 3** Implementation of DASGO (Diagonal Adaptive Structured Gradient Optimization)

---

- 1: **Input:**  $W_0 \in \mathbb{R}^{m \times n}$ ,  $\epsilon \in \mathbb{R}$ , lr schedule  $\{\eta_t\}$ , momentums  $\beta_1, \beta_2 \in [0, 1)$ , and batch size  $M \in \mathbb{N}$
  - 2: Initialize  $M_{-1} = 0 \in \mathbb{R}^{m \times n}$ ,  $v_{-1} = 0 \in \mathbb{R}^n$
  - 3: **for**  $t = 0$  **to**  $T - 1$  **do**
  - 4:   Sample mini-batch  $\mathcal{B}_t$  with  $|\mathcal{B}_t| \equiv M$  uniformly
  - 5:    $G_t = \frac{1}{M} \sum_{\xi \in \mathcal{B}_t} \nabla_W f(W_t; \xi)$
  - 6:    $M_t = \beta_1 M_{t-1} + (1 - \beta_1) G_t$
  - 7:    $v_t = \beta_2 v_{t-1} + (1 - \beta_2) \text{diag}(G_t^\top G_t)$
  - 8:    $W_{t+1} = W_t - \eta_t M_t \text{diag}(v_t + \epsilon)^{-\frac{1}{2}}$
  - 9: **end for**
- 

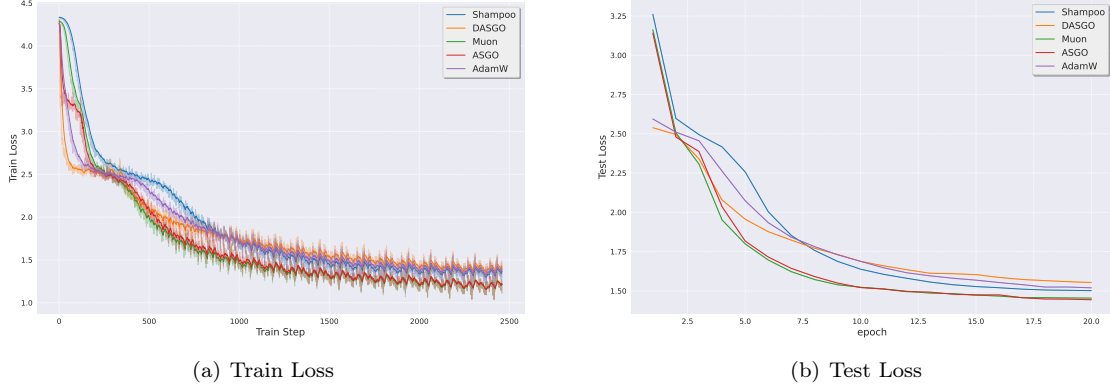


Figure 5: Train Loss and Test Loss on the NanoGPT and Shakespeare Character Dataset

attention heads, and an embedding dimension of 384, on the Shakespeare character-level dataset with a sequence length of 256 tokens. For all algorithms, we trained the model for 20 epochs, where each epoch contained 128 steps, using a batch size 128 and the OneCycle learning rate (lr) schedule.

Before discussing hyperparameter (HP) tuning, we note that recent research [Shi et al., 2023, Morwani et al., 2024, Lin et al., 2024] has suggested treating the inverse order (IO) in Shampoo’s preconditioner as a tunable HP rather than using the standard value of  $-1/4$ . Notably, Morwani et al. [2024] demonstrated that Shampoo with  $\text{IO} = -1/2$  provides a superior approximation of the full-matrix AdaGrad optimizer. Consequently, we treated the IO as a Shampoo HP in our pretraining experiments. Additionally, Shampoo’s performance is highly dependent on the initialization of its preconditioner matrices, as this is crucial for accurately approximating the Empirical Fisher Information Matrix [Morwani et al., 2024]. To address this initialization sensitivity, we implemented a preconditioner warmup phase specifically for Shampoo. Following the methodology in Ren and Goldfarb [2021], we dedicated the first epoch exclusively to accumulating statistics for the preconditioner matrices without updating model parameters. This approach yields a more robust estimation of the preconditioner, which significantly improves the stability of Shampoo during subsequent training iterations. Figure 5 depicts the training loss and validation loss for training NanoGPT with Shampoo, DASGO, Muon, ASGO and Adam-W.

**Hyperparameter Tuning** For consistency across all optimization methods, we employ the OneCycleLR learning rate schedule, which has been shown to provide stable convergence properties in deep learning tasks. To ensure optimal performance for each optimizer, we conducted a comprehensive HP search using random search [Bergstra and Bengio, 2012, Choi et al., 2019] within the following predefined ranges: initial lr:  $[10^{-5}, 10^{-1}]$ ;  $\beta_1$ :  $[0.7, 0.99]$ ;  $\beta_2$ :  $[0.7, 0.99]$ ; and selected the warmup factor from the set  $[0.1, 0.15, 0.2, 0.25, 0.3]$ . For the optimizers Shampoo and ASGO, we selected the update frequency  $\tau$  from the set  $[5, 10, 15]$  and for Shampoo, we selected its IO as either  $-1/2$  or  $-1/4$ . HPs were selected based on validation loss after 20 epochs of training. For each optimizer, we performed a random search for 16 hours to find the optimal HP combination. These best HP choices for training NanoGPT are given in Table 3.

Table 3: Hyperparameter selection for NanoGPT experiment

Optimizer	learning rate	$\beta_1$	$\beta_2$	warmup factor	update frequency	inverse order
Muon	0.00349	0.9881	N/A	0.3	N/A	N/A
AdamW	0.00450	0.9332	0.9528	0.2	N/A	N/A
DASGO	0.060	0.9584	0.9435	0.2	N/A	N/A
Shampoo	0.00593	0.9402	0.9760	0.3	15	$-\frac{1}{4}$
ASGO	0.01470	0.9541	0.8487	0.3	15	N/A

**Ablation Study: Impact of Special Query/Key Design** In Appendix B, we highlighted the computational benefits of specialized processing for Query and Key matrices in Transformer architectures. To validate these theoretical advantages empirically, we conducted an ablation study comparing the performance and training stability of ASGO and Muon on pretraining NanoGPT, both with and without the specialized Query-Key processing. We maintained the optimal HP configuration established in Table 3 for all parameters except the learning rate. For each algorithm variant (with and without specialized processing), we randomly sampled learning rates from a log-uniform distribution ranging from  $10^{-5}$  to  $10^{-1}$ . Each configuration was trained for 5 epochs on the NanoGPT model, after which we recorded the validation loss. This approach allowed us to evaluate both performance and robustness to learning rate selection. Figure 6 presents the distribution of validation losses after 5 epochs for both algorithms. The violin plots<sup>4</sup> reveal several key insights: (1) For ASGO (Figure 6a), the benefits of specialized Query-Key processing are substantial. The specialized implementation demonstrates a narrower, lower distribution of validation losses (centered around 2.5), indicating greater stability across different learning rates. In contrast, the vanilla implementation shows a long-tailed distribution extending beyond loss values of 6.0, with several outliers representing training instability at certain learning rates. (2) For Muon (Figure 6b), both implementations demonstrate nearly identical performance distributions, with their median validation losses and distribution shapes showing minimal differences. However, the specialized implementation achieves this comparable performance while reducing memory requirements and computational complexity. This represents a clear efficiency advantage – the specialized Query-Key processing effectively provides computational savings with no performance penalty.

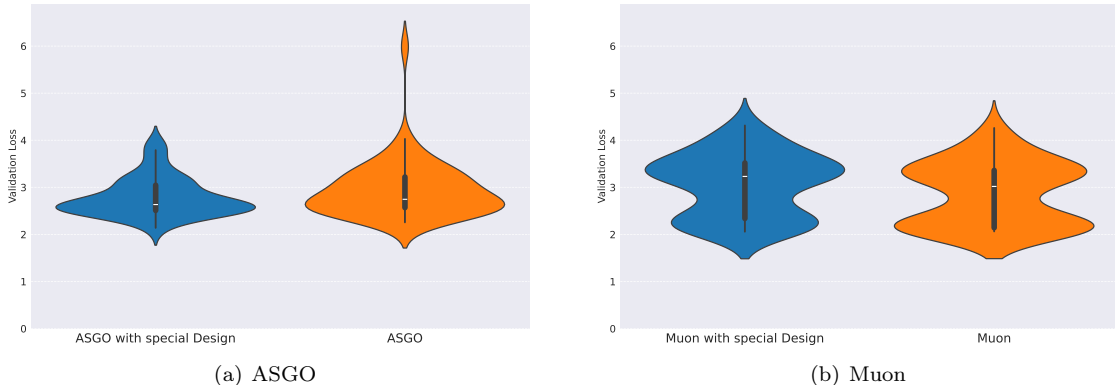


Figure 6: Distribution of validation losses after 5 epochs with varying learning rates.

## C.2 Pretraining GPT2

**Experimental Setup:** The model configuration consists of 12 Transformer layers, 12 attention heads, and an embedding dimension of 768. The total number of training steps was 1000, with a batch size per GPU of 32. The model was trained using Distributed Data Parallel (DDP) on 4 NVIDIA V100 GPUs, employing gradient accumulation over 8 steps. To ensure a fair comparison across all optimization algorithms, a consistent learning rate schedule was utilized: a linear warmup for the first 200 steps, followed by a cosine annealing decay to a final learning rate of  $1 \times 10^{-5}$  for the remainder of

<sup>4</sup>Violin plot outlines depict empirical probability density; i.e., the width of the shaded area represents the proportion of the data located there. Box plots within a violin plot display the median and inter-quartile range.

the training process. Training was conducted on the OpenWebText dataset with a sequence length of 512 tokens.

**Hyperparameter Tuning:** To ensure optimal performance for each optimizer, we conducted a hyperparameter search using grid search. The search space for learning rate (lr) and 2nd momentum  $\beta_2$  (where applicable for the optimizer) included the following values:

- Learning rate (lr):  $[1 \times 10^{-5}, 1 \times 10^{-4}, 5 \times 10^{-4}, 1 \times 10^{-3}, 5 \times 10^{-3}, 1 \times 10^{-2}, 5 \times 10^{-2}, 0.1, 0.5]$
- $\beta_2$ :  $[0.7, 0.8, 0.9, 0.95, 0.99]$

Optimal hyperparameters were selected based on the validation loss achieved after 1000 training steps. The best hyperparameter choices for pretraining GPT-2 are presented in Table 4.

Table 4: Optimal hyperparameter selection for pretraining GPT-2.

Optimizer	Learning Rate	$\beta_1$	$\beta_2$	Damping $\epsilon$	Update Freq. ( $\tau$ )
Muon	0.01	0.9	N/A	N/A	N/A
AdamW	0.005	0.9	0.99	$1 \times 10^{-6}$	N/A
DASGO	0.01	0.9	0.99	$1 \times 10^{-6}$	N/A
ASGO	0.1	0.9	0.95	$1 \times 10^{-6}$	1

### C.3 Finetune GPT2-Large

**Experimental Setup:** We fine-tuned the GPT-2 Large model on the WikiText-2 dataset. We utilized the GPT-2 Large model, which comprises approximately 774 million parameters. This model is a transformer-based language model pretrained on English text using a Causal Language Modeling (CLM) objective, initially developed by OpenAI and was accessed via the Hugging Face Hub. The fine-tuning was performed on the WikiText-2 dataset, a standard benchmark for evaluating language model performance. The dataset was loaded directly using standard library functions. We investigated two distinct fine-tuning objectives:

- Causal Language Modeling (CLM): The conventional autoregressive language modeling task.
- Fill-in-the-Middle (FIM): Adopting the methodology from Bavarian et al. (2022). This objective trains the model to infill masked text spans within a document.

All models were fine-tuned for a total of 2 epochs. For the learning rate, we employed a cosine annealing decay schedule over the course of these 2 epochs, with the learning rate decaying to 0 by the end of training. No warmup phase was used for the fine-tuning learning rate schedule. The fine-tuning process used a batch size of 16 and a sequence length of 128 tokens. For each optimizer evaluated (AdamW, Muon, ASGO, and DASGO), all hyperparameters, with the exception of the learning rate, were maintained at the same values used in our GPT-2 pretraining experiments (as detailed in Table 4).

**Hyperparameter Tuning:** For the fine-tuning experiments on WikiText-2, our hyperparameter tuning focused exclusively on identifying the optimal learning rate for each optimizer under both the CLM and FIM objectives. We performed a grid search over a predefined set of learning rate candidates:  $[1 \times 10^{-6}, 5 \times 10^{-5}, 1 \times 10^{-4}, 5 \times 10^{-4}, 1 \times 10^{-3}, 5 \times 10^{-3}]$ . The optimal learning rate for each optimizer and fine-tuning objective combination was determined by selecting the learning rate that yielded the lowest validation perplexity on the WikiText-2 validation set after the full 2 epochs of fine-tuning. Table 5 shows the optimal learning rate.

Table 5: Optimal Learning rate from Finetuning GPT2-Large

	AdamW	Muon	ASGO	DASGO
CLM	$5 \times 10^{-5}$	$5 \times 10^{-4}$	$1 \times 10^{-3}$	$1 \times 10^{-3}$
FIM	$1 \times 10^{-4}$	$5 \times 10^{-4}$	$1 \times 10^{-3}$	$1 \times 10^{-3}$

Table 6 presents the average perplexity results obtained after fine-tuning the GPT2-Large (774M) model for 2 epochs on the WikiText-2 dataset. The  $\pm$  indicates the 95% confidence intervals of the mean perplexity value over these 5 runs, starting from different random seeds.

Table 6: Finetuning GPT2-Large Perplexity				
	AdamW	Muon	ASGO	DASGO
CLM	$14.010 \pm 0.016$	$13.912 \pm 0.003$	$13.879 \pm 0.010$	$13.841 \pm 0.019$
FIM	$17.458 \pm 2.254$	$15.933 \pm 0.102$	$15.661 \pm 0.097$	$15.451 \pm 0.072$

**Damping parameter  $\epsilon$  sensitivity study:** In this section, we discuss the practical differences between ASGO and Muon. Theoretically, as discussed in Section 6, ASGO can be viewed as an adaptive extension of Muon. Specifically, ASGO’s update rule degenerates to that of Muon in the absence of momentum and adaptive scaling (i.e., when  $\beta_1 = 0$  and  $\beta_2 = 0$ ).

Moreover, if we modify the formulas for  $V_t$  and  $W_{t+1}$  in ASGO (Algorithm 2) to:

$$\begin{aligned}
&\text{if } m < n \text{ then } V_t = \beta_2 V_{t-1} + (1 - \beta_2) M_t M_t^\top \\
&\text{else } V_t = \beta_2 V_{t-1} + (1 - \beta_2) M_t^\top M_t \\
&\text{if } m < n \text{ then } W_{t+1} = W_t - \eta_t (V_t + \epsilon I)^{-\frac{1}{2}} M_t \\
&\text{else } W_{t+1} = W_t - \eta_t M_t (V_t + \epsilon I)^{-\frac{1}{2}}
\end{aligned} \tag{4}$$

and set  $\beta_2 = 0$  ASGO becomes identical to Muon, even with momentum. However, in practical training implementations, a subtle yet crucial difference exists between ASGO and Muon. This distinction arises because ASGO applies an additional preconditioner with  $\epsilon$  damping to the momentum term, a step not present in the standard Muon update.

To precisely study these differences, we set up an experiment using the Muon optimizer as the background optimizer to train a GPT2-model on the NanoGPT dataset for 1000 steps. At each step, we computed and compared the Muon and ASGO update directions  $\Delta W$  in the embedding, query, key, value, and MLP layers. Specifically, we computed:

- **Standard Muon Update Direction (SVD-based):**  $\Delta W_{\text{SVD}}^{\text{Muon}} = U_M V_M^T$ , where  $U_M$  and  $V_M$  are the left and right singular vectors obtained from the first-order momentum  $M$ .
- **Modified ASGO Update Direction (SVD-based,  $\epsilon = 0$ ):**  $\Delta W_{\text{SVD}, \epsilon=0}^{\text{ASGO}} = V_t^{-\frac{1}{2}} M_t$ , where  $V_t^{-\frac{1}{2}}$  is computed via standard Singular Value Decomposition (SVD).
- **Modified ASGO Update Direction (SVD-based,  $\epsilon = 10^{-8}$ ):**  $\Delta W_{\text{SVD}, \epsilon=10^{-8}}^{\text{ASGO}} = (V_t + 10^{-8} I)^{-\frac{1}{2}} M_t$ , where  $(V_t + 10^{-8} I)^{-\frac{1}{2}}$  is computed via standard SVD.
- **Modified ASGO Update Direction (Coupled Newton,  $\epsilon = 10^{-8}$ ):**  $\Delta W_{\text{CN}, \epsilon=10^{-8}}^{\text{ASGO}} = (V_t + 10^{-8} I)^{-\frac{1}{2}} M_t$ , where  $(V_t + 10^{-8} I)^{-\frac{1}{2}}$  is computed using the Coupled Newton algorithm for 50 iteration steps. Higham [2008], Shi et al. [2023]
- **Modified ASGO Update Direction (Newton-Schulz,  $\epsilon = 10^{-8}$ ):**  $\Delta W_{\text{NS}, \epsilon=10^{-8}}^{\text{ASGO}} = (V_t + 10^{-8} I)^{-\frac{1}{2}} M_t$ , where  $(V_t + 10^{-8} I)^{-\frac{1}{2}}$  is computed using the Newton-Schulz algorithm for 50 iteration steps.<sup>5</sup> Higham [2008], Bernstein and Newhouse [2024b], Jordan et al. [2024]

We then computed the cosine similarity<sup>6</sup> between each of the four modified ASGO update directions and the standard Muon update direction  $\Delta W_{\text{SVD}}^{\text{Muon}}$ , and plotted these similarities in Figure 7.

Unlike AdamW, ASGO exhibits sensitivity to the choice of the  $\epsilon$  damping parameter. As depicted in Figure 7(a), when no damping term is used ( $\epsilon = 0$ ), ASGO’s update direction, though exhibiting some

<sup>5</sup>The Newton-Schulz algorithm is derived from Algorithm 6.35 on Page 153 in Higham [2008]. We utilized the quintic version with parameters  $(a, b, c) = (2, -1.5, 0.5)$  as described in Jordan et al. [2024].

<sup>6</sup>CosineSimilarity( $A, B$ ) =  $\frac{\text{Tr}(A^T B)}{\|A\|_F \|B\|_F}$

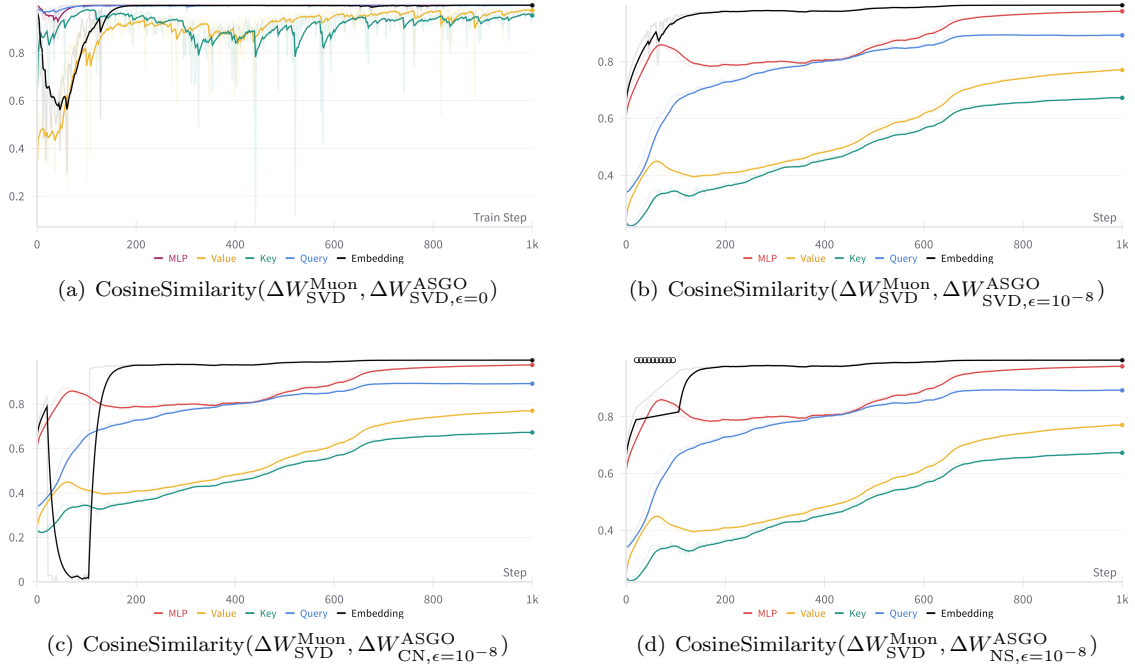


Figure 7: Comparison of Cosine Similarities (CSs) between the Muon update direction ( $\Delta W_{\text{SVD}}^{\text{Muon}}$ ) and various modified ASGO update directions in different layers (MLP, Value, Key, Query, Embedding) during 1000 steps of GPT2 pretraining. Subfigures (a) and (b) plot CSs for SVD-based ASGO update directions with  $\epsilon = 0$  and  $\epsilon = 10^{-8}$ , respectively. Subfigure (c) and (d) plot CSs for Coupled Newton-based and Newton-Schulz-based, respectively, ASGO update directions with  $\epsilon = 10^{-8}$ .

instability, largely reconstructs Muon’s update direction, with cosine similarities generally exceeding 0.8, particularly for the MLP and Embedding layers, as training progresses. However, the introduction of a small damping hyperparameter ( $\epsilon = 10^{-8}$ ) significantly alters these similarities. Figure 7(b) shows that even with precise SVD computation, the similarities for layers like Value and Key only reach approximately 0.7 gradually. This suggests that the small  $\epsilon$  value can introduce and accumulate errors during training, potentially leading to a degradation in optimizer performance, a behavior not typically observed in other common adaptive methods like AdamW. This phenomenon highlights the critical importance of small singular values in the preconditioning process, as applying a damping term can disproportionately affect them, thereby altering the matrix multiplication and amplifying errors. To circumvent this sensitivity, we opted to use an  $\epsilon$  value of 0 in our large-scale GPT2 pretraining experiments described in Section 7.2. In this setting, we directly compute the SVD of the preconditioning matrix and its inverse square root. The results presented in Figure 2 indeed demonstrate that ASGO achieves performance highly similar to Muon.

In Figure 7(c) and (d), we explore the use of more computationally efficient methods, Coupled Newton (CN) and Newton-Schulz (NS), respectively, to approximately compute  $V_t^{-\frac{1}{2}}$  as alternatives to SVD. The results show that, aside from some numerical stability issues observed in the Embedding layer for both CN and NS at certain steps—which is reasonable given that the sparse nature of embedding layers often requiring larger damping parameters—the cosine similarities for the remaining parameters are highly comparable to those obtained with SVD. This demonstrates the feasibility of employing efficient matrix algorithms to replace SVD, thereby enhancing ASGO’s computational efficiency. This direction represents one of our promising avenues for future research.

## D Auxiliary Lemmas for the Proof

**Lemma 1** (Trace properties). *For arbitrary matrices  $A \in \mathbb{R}^{m \times n}$ ,  $B \in \mathbb{R}^{n \times m}$ ,  $X, Y \in \mathbb{R}^{m \times m}$ , we have the following basic properties for the trace:*

1.  $\text{tr}(X) = \text{tr}(X^\top)$ ;

2.  $\text{tr}(AB) = \text{tr}(BA)$ ;
3. if  $X$  is symmetric positive semidefinite,  $\text{tr}(X) = \|X\|_* \geq 0$ ;
4. if  $X, Y \succeq 0$  and  $X$  is symmetric,  $\text{tr}(XY) \geq 0$ .

The following lemma notes the operator monotonicity of the power functions, which is a classic result [Löwner, 1934, Ando et al., 2004, Gupta et al., 2018].

**Lemma 2.** *The function  $f : x \rightarrow x^\alpha$  with  $\alpha \in [0, 1]$  is operator-monotone, i.e. if  $0 \preceq A \preceq B$ , it holds that  $A^\alpha \preceq B^\alpha$ .*

**Lemma 3.** *For symmetric positive definite matrices  $X, Y \in \mathbb{R}^{m \times m}$ , it holds that*

$$\text{tr}\left((X + Y)^{\frac{1}{2}}\right) \leq \text{tr}\left(X^{\frac{1}{2}} + Y^{\frac{1}{2}}\right).$$

*Proof.* It holds that

$$\begin{aligned} \text{tr}\left((X + Y)^{\frac{1}{2}}\right) &= \text{tr}\left((X + Y)^{-\frac{1}{2}}(X + Y)\right) \\ &= \text{tr}\left((X + Y)^{-\frac{1}{2}}X\right) + \text{tr}\left((X + Y)^{-\frac{1}{2}}Y\right) \\ &\geq \text{tr}\left(X^{\frac{1}{2}}\right) + \text{tr}\left(Y^{\frac{1}{2}}\right), \end{aligned}$$

where the last inequality is based on Lemma 2 such that  $(X + Y)^{\frac{1}{2}} \succeq X^{\frac{1}{2}}$  and the fact that  $A^{-1} \preceq B^{-1}$  if  $A \succeq B$  for symmetric positive definite matrices  $A, B$ . Further based on Lemma 1, we can finish the proof.  $\square$

**Lemma 4.** *For a symmetric positive semidefinite matrix  $X \in \mathbb{R}^{m \times m}$ , it holds that*

$$\text{tr}\left(X^{\frac{1}{2}}\right) \leq \sum_{j=1}^m \sqrt{[X]_{j,j}}.$$

*Proof.* The inequality is equivalent to that

$$\sum_{i=1}^m \sqrt{\lambda_i(X)} \leq \sum_{i=1}^m \sqrt{[X]_{i,i}},$$

where  $\lambda_i(X)$  denotes the  $i$ -th largest eigenvalue of  $X$  (the same as singular values for real symmetric positive semidefinite matrices). Firstly, we have the fact that the eigenvalues  $\{\lambda_i(X)\}_{i=1}^m$  majorize the diagonal entries  $\{[X]_{i,i}\}_{i=1}^m$ , i.e. for all  $1 \leq l < m$ ,

$$\sum_{i=1}^l \lambda_i(X) \geq \sum_{i=1}^l [X]_{i,i}, \quad \text{and} \quad \sum_{i=1}^m \lambda_i(X) = \sum_{i=1}^m [X]_{i,i}.$$

Also, we know  $g : \{x_i\}_{i=1}^m \rightarrow \sum_{i=1}^m x_i^{\frac{1}{2}}$  is a Schur-concave operator. Then we obtain the equality based on the Schur-Horn theorem, which implies that for a Schur-concave operator  $g$ , if sequence  $\{x_i\}_{i=1}^m$  majorizes  $\{y_i\}_{i=1}^m$ , then  $g(\{x_i\}_{i=1}^m) \leq g(\{y_i\}_{i=1}^m)$ .  $\square$

**Lemma 5.**  $\|\cdot\|_L$  is a norm, i.e., it satisfies the basic properties of norms. Its dual norm is  $\|\cdot\|_{L^{-1}}$ .

*Proof.* Denote  $X = [x_1, \dots, x_n] \in \mathbb{R}^{m \times n}$ , where each  $x_i \in \mathbb{R}^{1 \times m}$ . Then we have

$$\text{tr}(X^\top LX) = \sum_{i=1}^n x_i^\top L x_i = \begin{bmatrix} x_1 \\ \vdots \\ x_n \end{bmatrix}^\top \begin{bmatrix} L & & \\ & \ddots & \\ & & L \end{bmatrix} \begin{bmatrix} x_1 \\ \vdots \\ x_n \end{bmatrix},$$

which is a norm for the space  $\mathbb{R}^{m \times n}$  whose dual norm is  $\|\cdot\|_{L^{-1}}$ . This concludes the proof.  $\square$

**Lemma 6.** Assume a non-negative sequence  $\{x_j\}_{j=1}^n$  and a positive sequence  $\{s_j\}_{j=1}^n$  with  $S = \sum_{i=1}^n s_j$ , it holds that

$$\frac{1}{S} \sum_{j=1}^n x_j \leq \sqrt{\frac{1}{S} \sum_{j=1}^n \frac{x_j^2}{s_j}}. \quad (5)$$

The inequality holds as an equality if and only if for all  $i = 1, \dots, n$  and  $j = 1, \dots, n$ ,

$$\frac{x_i}{s_i} = \frac{x_j}{s_j}.$$

*Proof.* A proof can be found in Lemma G.5 of the ICLR version of Liu et al. [2024].  $\square$

## E Proof of Nonsmooth Convergence of ASGO

*Proof of Theorem 1.* Denote  $\Delta W_t \triangleq W_t - W_*$  where  $W_*$  is an optimum of Problem (1). From the algorithm update, we have

$$\Delta W_{t+1}^\top \Lambda_t \Delta W_{t+1} = \Delta W_t^\top \Lambda_t \Delta W_t - \eta_t (G_t^\top \Delta W_t + \Delta W_t^\top G_t) + \eta_t^2 G_t^\top \Lambda_t^{-1} G_t.$$

Then, by taking trace of the above equality and rearranging, we can obtain that

$$2\eta_t \text{tr}(G_t^\top \Delta W_t) = \text{tr}(\Delta W_t^\top \Lambda_t \Delta W_t - \Delta W_{t+1}^\top \Lambda_t \Delta W_{t+1}) + \eta_t^2 \text{tr}(G_t^\top \Lambda_t^{-1} G_t).$$

By convexity, we know

$$\mathbb{E}[\text{tr}(G_t^\top \Delta W_t)] = \mathbb{E}[\langle \nabla f(W_t), \Delta W_t \rangle] \geq \mathbb{E}[f(W_t)] - f(W_*).$$

Then combining these and taking summation over  $t$  and taking  $\eta_t \equiv \eta$ , we have

$$\begin{aligned} & 2 \sum_{t=0}^{T-1} \mathbb{E}[f(W_t)] - f(W_*) \\ & \leq \frac{1}{\eta} \mathbb{E} \left[ \sum_{t=0}^{T-1} \text{tr}(\Delta W_t^\top \Lambda_t \Delta W_t - \Delta W_{t+1}^\top \Lambda_t \Delta W_{t+1}) \right] + \eta \mathbb{E} \left[ \sum_{t=0}^{T-1} \text{tr}(G_t^\top \Lambda_t^{-1} G_t) \right] \\ & = \frac{1}{\eta} \mathbb{E} \left[ \sum_{t=0}^{T-1} \text{tr}(\Delta W_t^\top \Lambda_t \Delta W_t - \Delta W_t^\top \Lambda_{t-1} \Delta W_t) \right] + \frac{1}{\eta} \text{tr}(\Delta W_0^\top \Lambda_{-1} \Delta W_0) - \frac{1}{\eta} \mathbb{E}[\text{tr}(\Delta W_T^\top \Lambda_{T-1} \Delta W_T)] \\ & \quad + \eta \mathbb{E} \left[ \sum_{t=0}^{T-1} \text{tr}(G_t^\top \Lambda_t^{-1} G_t) \right] \\ & \leq \frac{1}{\eta} \text{tr}(\Delta W_0^\top \Lambda_{-1} \Delta W_0) + \frac{1}{\eta} \mathbb{E} \left[ \sum_{t=0}^{T-1} \text{tr}(\Delta W_t^\top (\Lambda_t - \Lambda_{t-1}) \Delta W_t) \right] + \eta \mathbb{E} \left[ \sum_{t=0}^{T-1} \text{tr}(G_t^\top \Lambda_t^{-1} G_t) \right], \end{aligned} \quad (6)$$

where we note  $\Lambda_{-1} = \epsilon I_m$ . Thus the first term on the RHS of (6) can be bounded by  $\epsilon$  as

$$\frac{1}{\eta} \text{tr}(\Delta W_0^\top \Lambda_{-1} \Delta W_0) = \frac{\epsilon}{\eta} \|\Delta W_0\|_F^2 \leq \frac{\epsilon D_F^2}{\eta}. \quad (7)$$

We then deal with the second and third terms separately. For the second term, we have

$$\begin{aligned} \sum_{t=0}^{T-1} \text{tr}(\Delta W_t^\top (\Lambda_t - \Lambda_{t-1}) \Delta W_t) &= \sum_{t=0}^{T-1} \text{tr}(\Delta W_t \Delta W_t^\top (\Lambda_t - \Lambda_{t-1})) \\ &= \sum_{t=0}^{T-1} \langle \Delta W_t \Delta W_t^\top, \Lambda_t - \Lambda_{t-1} \rangle \\ &\leq \sum_{t=0}^{T-1} \|\Delta W_t \Delta W_t^\top\|_{\text{op}} \|\Lambda_t - \Lambda_{t-1}\|_* \\ &= \sum_{t=0}^{T-1} \|\Delta W_t\|_{\text{op}}^2 \text{tr}(\Lambda_t - \Lambda_{t-1}) \leq D_{\text{op}}^2 \text{tr}(\Lambda_{T-1} - \text{tr}(\Lambda_{-1})). \end{aligned} \quad (8)$$

Note that the first and last equalities are based on the properties of the trace, (see Lemma 1). The first inequality is based on the duality of the  $\|\cdot\|_{\text{op}}$  and  $\|\cdot\|_*$  norms. The third equality relies on the positive semidefiniteness of  $\Lambda_t - \Lambda_{t-1}$  for all  $t$  based on Lemma 2, since  $\Lambda_t^2 - \Lambda_{t-1}^2 = G_t G_t^\top \succeq 0$ .

For the third term of (6), we have

$$\begin{aligned} \text{tr}(G_t^\top \Lambda_t^{-1} G_t) &= \text{tr}(G_t G_t^\top \Lambda_t^{-1}) = \text{tr}((\Lambda_t^2 - \Lambda_{t-1}^2) \Lambda_t^{-1}) \\ &= \text{tr}((\Lambda_t - \Lambda_{t-1}) \cdot 2\Lambda_t - (\Lambda_t - \Lambda_{t-1})^2 + \Lambda_{t-1} \Lambda_t - \Lambda_t \Lambda_{t-1}) \Lambda_t^{-1}) \\ &= 2\text{tr}(\Lambda_t - \Lambda_{t-1}) - \text{tr}((\Lambda_t - \Lambda_{t-1})^2 \Lambda_t^{-1}) + \text{tr}((\Lambda_{t-1} \Lambda_t - \Lambda_t \Lambda_{t-1}) \Lambda_t^{-1}) \\ &\leq 2\text{tr}(\Lambda_t - \Lambda_{t-1}), \end{aligned} \tag{9}$$

where the last inequality follows from the fact that

$$\text{tr}((\Lambda_t - \Lambda_{t-1})^2 \Lambda_t^{-1}) = \text{tr}\left(\left[(\Lambda_t - \Lambda_{t-1}) \Lambda_t^{-\frac{1}{2}}\right] \left[(\Lambda_t - \Lambda_{t-1}) \Lambda_t^{-\frac{1}{2}}\right]^\top\right) \geq 0$$

and

$$\text{tr}((\Lambda_{t-1} \Lambda_t - \Lambda_t \Lambda_{t-1}) \Lambda_t^{-1}) = \text{tr}(\Lambda_{t-1}) - \text{tr}(\Lambda_t \Lambda_{t-1} \Lambda_t^{-1}) = 0,$$

which are based on the positive definiteness of  $\Lambda_t$  and the properties of the trace (Lemma 1). Therefore, by substituting (7), (8), and (9) into (6), we have

$$\begin{aligned} &2 \sum_{t=0}^{T-1} \mathbb{E}[f(W_t)] - f(W_*) \\ &\leq \frac{1}{\eta} \text{tr}(\Delta W_0^\top \Lambda_{-1} \Delta W_0) + \frac{1}{\eta} \mathbb{E} \left[ \sum_{t=0}^{T-1} \text{tr}(\Delta W_t^\top (\Lambda_t - \Lambda_{t-1}) \Delta W_t) \right] + \eta \mathbb{E} \left[ \sum_{t=0}^{T-1} \text{tr}(G_t^\top \Lambda_t^{-1} G_t) \right] \\ &\leq \frac{\epsilon D_F^2}{\eta} + \left( \frac{D_{\text{op}}^2}{\eta} + 2\eta \right) \mathbb{E}[\text{tr}(\Lambda_{T-1} - \Lambda_{-1})] \\ &= \left( \frac{D_{\text{op}}^2}{\eta} + 2\eta \right) \mathbb{E} \left[ \text{tr} \left( \left( \sum_{t=0}^{T-1} G_t G_t^\top \right)^{\frac{1}{2}} \right) \right] + \frac{\epsilon D_F^2}{\eta}. \end{aligned}$$

Taking  $\eta = D_{\text{op}}$  completes the proof.  $\square$

Based on Theorem 1 and Lemma 8, we can also prove Corollary 2.

*Proof of Corollary 2.* Based on the results in Theorem 1, if we additionally have

$$\mathbb{E}[G_t G_t^\top] \preceq Q^2,$$

then using Lemma 8, we can obtain that

$$\begin{aligned} \mathbb{E} \left[ \left\| \left( \sum_{t=0}^{T-1} G_t G_t^\top \right)^{\frac{1}{2}} \right\|_* \right] &\stackrel{(10)}{\leq} \mathbb{E} \left[ \sqrt{\|Q\|_* \text{tr} \left( \left( \sum_{t=0}^{T-1} G_t G_t^\top \right)^{\frac{1}{2}} Q^{-1} \left( \sum_{t=0}^{T-1} G_t G_t^\top \right)^{\frac{1}{2}} \right)} \right] \\ &= \mathbb{E} \left[ \sqrt{\|Q\|_* \text{tr} \left( \sum_{t=0}^{T-1} G_t G_t^\top Q^{-1} \right)} \right] \\ &\leq \sqrt{\|Q\|_* \sum_{t=0}^{T-1} \text{tr}(\mathbb{E}[G_t G_t^\top] Q^{-1})} \\ &\leq \sqrt{\|Q\|_* \sum_{t=0}^{T-1} \|Q\|_*} = \sqrt{T} \|Q\|_*, \end{aligned}$$

where the first equality is based on Lemma 1 and the second inequality is based on the fact that  $g(x) = \sqrt{x}$  is concave for  $x \geq 0$ . This concludes the proof.  $\square$

We also provide the following proof for the comparison between Theorem 1 and the convergence rates of Shampoo and full-matrix AdaGrad.

*Proof of Comparison with Shampoo and full-matrix AdaGrad.* We list the convergence rates here.

$$\text{Full-Matrix AdaGrad: } \mathcal{O} \left( D_F \sum_{j=1}^m \sum_{i=1}^n \sqrt{\sum_{t=0}^{T-1} [G_t]_{i,j}^2} \right)$$

$$\text{Shampoo: } \mathcal{O} \left( \sqrt{r_G} D_F \cdot \text{tr} \left( \left( \sum_{t=0}^{T-1} G_t G_t^\top \right)^{\frac{1}{4}} \right) \cdot \text{tr} \left( \left( \sum_{t=0}^{T-1} G_t^\top G_t \right)^{\frac{1}{4}} \right) \right)$$

$$\text{ASGO: } \mathcal{O} \left( D_{\text{op}} \cdot \text{tr} \left( \left( \sum_{t=0}^{T-1} G_t G_t^\top \right)^{\frac{1}{2}} \right) \right) \leq \mathcal{O} \left( D_{\text{op}} \right)$$

The last inequality for ASGO is based on Lemma 4. We first compare ASGO and full-matrix AdaGrad:

$$\text{tr} \left( \left( \sum_{t=0}^{T-1} G_t G_t^\top \right)^{\frac{1}{2}} \right) \leq \sum_{j=1}^m \sqrt{\left[ \sum_{t=0}^{T-1} G_t G_t^\top \right]_{j,j}} = \sum_{j=1}^m \sqrt{\sum_{i=1}^n \sum_{t=0}^{T-1} [G_t]_{i,j}^2} \leq \sum_{j=1}^m \sum_{i=1}^n \sqrt{\sum_{t=0}^{T-1} [G_t]_{i,j}^2},$$

where the first inequality is based on Lemma 4 and the second inequality is simply a fact that for any vector  $x$ , we have  $\|x\|_2 \geq \|x\|_1$ . Thus we prove that the proven convergence rate of ASGO is at least  $D_F/D_{\text{op}}$  times faster than full-matrix AdaGrad.

Then we compare ASGO and Shampoo. We have

$$\begin{aligned} \text{tr} \left( \left( \sum_{t=0}^{T-1} G_t G_t^\top \right)^{\frac{1}{2}} \right) &= \left\langle \left( \sum_{t=0}^{T-1} G_t G_t^\top \right)^{\frac{1}{4}}, \left( \sum_{t=0}^{T-1} G_t G_t^\top \right)^{\frac{1}{4}} \right\rangle \\ &\leq \text{tr} \left( \left( \sum_{t=0}^{T-1} G_t G_t^\top \right)^{\frac{1}{4}} \right) \cdot \left\| \left( \sum_{t=0}^{T-1} G_t G_t^\top \right)^{\frac{1}{4}} \right\|_{\text{op}} \\ &= \text{tr} \left( \left( \sum_{t=0}^{T-1} G_t G_t^\top \right)^{\frac{1}{4}} \right) \cdot \left\| \sum_{t=0}^{T-1} G_t G_t^\top \right\|_{\text{op}}^{\frac{1}{4}}, \end{aligned}$$

where the inequality is based on the fact that  $\|\cdot\|_{\text{op}}$  and  $\|\cdot\|_*$  are dual norms. Then we have

$$\begin{aligned} \left\| \sum_{t=0}^{T-1} G_t G_t^\top \right\|_{\text{op}}^{\frac{1}{4}} &\leq \left( \sum_{t=0}^{T-1} \|G_t G_t^\top\|_{\text{op}} \right)^{\frac{1}{4}} = \left( \sum_{t=0}^{T-1} \|G_t^\top G_t\|_{\text{op}} \right)^{\frac{1}{4}} \\ &\leq \left( \text{tr} \left( \sum_{t=0}^{T-1} G_t^\top G_t \right) \right)^{\frac{1}{4}} \leq \text{tr} \left( \left( \sum_{t=0}^{T-1} G_t^\top G_t \right)^{\frac{1}{4}} \right), \end{aligned}$$

where the first inequality is based on that  $\|\cdot\|_{\text{op}}$  is a norm and the second inequality is based on the fact that  $\text{tr}(X) \geq \|X\|_{\text{op}}$  for symmetric positive semidefinite  $X$ , and the third inequality is based on the fact that  $(\text{tr}(X))^{\frac{1}{4}} \leq \text{tr}(X^{\frac{1}{4}})$  because if we denote  $\sigma_j$  as the  $j$ -th singular value of  $X$ , we have

$$(\text{tr}(X))^{\frac{1}{4}} = \left( \sum_{j=1}^r \sigma_j \right)^{\frac{1}{4}} \leq \sum_{j=1}^r \sigma_j^{\frac{1}{4}}.$$

Thus we can conclude that

$$\text{tr} \left( \left( \sum_{t=0}^{T-1} G_t G_t^\top \right)^{\frac{1}{2}} \right) \leq \text{tr} \left( \left( \sum_{t=0}^{T-1} G_t G_t^\top \right)^{\frac{1}{4}} \right) \cdot \text{tr} \left( \left( \sum_{t=0}^{T-1} G_t^\top G_t \right)^{\frac{1}{4}} \right).$$

Therefore, the proven rate of ASGO is at least  $\sqrt{r_G} D_F/D_{\text{op}}$  times faster than Shampoo.  $\square$

## F Proof of Smooth Convergence of ASGO

The starting point of the smooth analysis is Theorem 1. For notation simplicity, we denote  $N_t \triangleq G_t - \nabla f(W_t)$  and  $\nabla f_t \triangleq \nabla f(W_t)$  in this section.

**Lemma 7** (Separate Gradient and Noise). *Under the same settings as Theorem 1, it holds that*

$$\frac{1}{T} \sum_{t=0}^{T-1} \mathbb{E}[f(W_t) - f(W_*)] \leq \frac{D_{\text{op}}}{T} \mathbb{E} \left[ \left\| \left( 2 \sum_{t=0}^{T-1} \nabla f_t \nabla f_t^\top \right)^{\frac{1}{2}} \right\|_* \right] + \frac{D_{\text{op}}}{T} \mathbb{E} \left[ \left\| \left( 2 \sum_{t=0}^{T-1} N_t N_t^\top \right)^{\frac{1}{2}} \right\|_* \right] + \frac{\epsilon D_F^2}{D_{\text{op}} T}.$$

*Proof.* Based on Theorem 1, we have

$$\begin{aligned} \frac{1}{T} \sum_{t=0}^{T-1} \mathbb{E}[f(W_t) - f(W_*)] &\leq \frac{D_{\text{op}}}{T} \mathbb{E} \left[ \left\| \left( \sum_{t=0}^{T-1} G_t G_t^\top \right)^{\frac{1}{2}} \right\|_* \right] + \frac{\epsilon D_F^2}{D_{\text{op}} T} \\ &\leq \frac{D_{\text{op}}}{T} \mathbb{E} \left[ \left\| \left( \sum_{t=0}^{T-1} 2 \nabla f_t \nabla f_t^\top + 2 N_t N_t^\top \right)^{\frac{1}{2}} \right\|_* \right] + \frac{\epsilon D_F^2}{D_{\text{op}} T} \\ &\leq \frac{D_{\text{op}}}{T} \mathbb{E} \left[ \left\| \left( 2 \sum_{t=0}^{T-1} \nabla f_t \nabla f_t^\top \right)^{\frac{1}{2}} \right\|_* \right] + \frac{D_{\text{op}}}{T} \mathbb{E} \left[ \left\| \left( 2 \sum_{t=0}^{T-1} N_t N_t^\top \right)^{\frac{1}{2}} \right\|_* \right] + \frac{\epsilon D_F^2}{D_{\text{op}} T}. \end{aligned}$$

Here the first inequality comes directly from Theorem 1. The second inequality is based on the fact that for all  $A, B \in \mathbb{R}^{m \times n}$  we have

$$\begin{aligned} 2AA^\top + 2BB^\top - (A+B)(A+B)^\top &= AA^\top + BB^\top - A^\top B - B^\top A \\ &= (A-B)(A-B)^\top \succeq 0. \end{aligned}$$

The last inequality is based on Lemma 3.  $\square$

The following lemma is a key technical lemma for proving the smooth convergence results, which is a generalization to the matrix case of Lemma 6.

**Lemma 8** (An upper bound on  $\|\cdot\|_*$ ). *For a symmetric positive definite matrix  $\Lambda \in \mathbb{R}^{m \times m}$  and matrix  $G \in \mathbb{R}^{m \times n}$ , it holds that*

$$\|G\|_* \leq \sqrt{\|\Lambda\|_* \text{tr}(G^\top \Lambda^{-1} G)}. \quad (10)$$

*Proof.* We first consider the case  $\Lambda = \text{diag}[\lambda_1, \dots, \lambda_m]$  is a diagonal matrix. We have

$$\begin{aligned} \|G\|_* &= \text{tr} \left( (GG^\top)^{\frac{1}{2}} \right) \leq \sum_{j=1}^m \sqrt{[GG^\top]_{j,j}} \\ &\leq \sqrt{\left( \sum_{j=1}^m \lambda_j \right) \left( \sum_{j=1}^m \frac{[GG^\top]_{j,j}}{\lambda_j} \right)} \\ &= \sqrt{\|\Lambda\|_* \text{tr}(GG^\top \Lambda^{-1})} = \sqrt{\|\Lambda\|_* \text{tr}(G^\top \Lambda^{-1} G)}, \end{aligned}$$

where the first inequality is based on Lemma 4 and the second inequality is based on Lemma 6.

Then we prove that this holds for general symmetric positive definite matrix  $\Lambda$ . Let the singular value decomposition be  $\Lambda = U \Sigma U^\top$ . Denote  $\tilde{G} = U^\top G$ . Since  $\Sigma \in \mathbb{R}^{m \times m}$  is a diagonal matrix, it holds that

$$\begin{aligned} \|G\|_* &= \|\tilde{G}\|_* \leq \sqrt{\|\Sigma\|_* \text{tr}(\tilde{G}^\top \Sigma^{-1} \tilde{G})} = \sqrt{\|\Lambda\|_* \text{tr}(G^\top U \Sigma^{-1} U^\top G)} \\ &= \sqrt{\|\Lambda\|_* \text{tr}(G^\top \Lambda^{-1} G)}, \end{aligned}$$

which concludes the proof.  $\square$

We also use the following lemma to indicate the reduction of variance by batch size  $M$ .

**Lemma 9** (Variance reduction by batch size). *Under Assumption 3, we have*

$$\mathbb{E} [N_t N_t^\top] \preceq \frac{1}{M} V^2,$$

where we denote  $N_t \triangleq G_t - \nabla f(W_t)$  for Algorithm 1.

*Proof.* For notation simplicity, we denote  $N(W_t; \xi) \triangleq \nabla f(W_t; \xi) - \nabla f(W_t)$  and thus

$$N_t = \frac{1}{M} \sum_{\xi \in \mathcal{B}} N(W_t; \xi).$$

Then it holds that

$$\begin{aligned} \mathbb{E} [N_t N_t^\top] &= \frac{1}{M^2} \mathbb{E} \left[ \left( \sum_{\xi \in \mathcal{B}} N(W_t; \xi) \right) \left( \sum_{\zeta \in \mathcal{B}} N(W_t; \zeta) \right)^\top \right] \\ &= \frac{1}{M^2} \sum_{\xi \in \mathcal{B}} \sum_{\zeta \in \mathcal{B}} \mathbb{E} [N(W_t; \xi) N(W_t; \zeta)^\top] \\ &= \frac{1}{M^2} \sum_{\xi \in \mathcal{B}} \mathbb{E} [N(W_t; \xi) N(W_t; \xi)^\top] \\ &\preceq \frac{1}{M^2} \sum_{\xi \in \mathcal{B}} V^2 = \frac{1}{M} V^2, \end{aligned}$$

where the last equality is based on that  $\nabla f(W_t; \xi)$  are mutually independent and  $\mathbb{E}[N(W_t; \xi)] = 0$  and the last inequality is based on Assumption 3.  $\square$

Then based on these lemmas, we can prove the smooth results.

*Proof of Theorem 3.* We separately deal with the bias and variance terms, which refer to the first two terms on the RHS of Lemma 7. For the bias part, by plugging in the smoothness matrix  $L$  into Lemma 8, we can obtain

$$\begin{aligned} \mathbb{E} \left[ \left\| \left( \sum_{t=0}^{T-1} \nabla f_t \nabla f_t^\top \right)^{\frac{1}{2}} \right\|_* \right] &\stackrel{(10)}{\leq} \mathbb{E} \left[ \sqrt{\|L\|_* \operatorname{tr} \left( \left( \sum_{t=0}^{T-1} \nabla f_t \nabla f_t^\top \right)^{\frac{1}{2}} L^{-1} \left( \sum_{t=0}^{T-1} \nabla f_t \nabla f_t^\top \right)^{\frac{1}{2}} \right)} \right] \\ &= \mathbb{E} \left[ \sqrt{\|L\|_* \operatorname{tr} \left( \sum_{t=0}^{T-1} \nabla f_t \nabla f_t^\top L^{-1} \right)} \right] \\ &\leq \sqrt{\|L\|_* \sum_{t=0}^{T-1} \mathbb{E} [\|\nabla f_t\|_{L^{-1}}^2]} \leq \sqrt{\|L\|_* \sum_{t=0}^{T-1} 2(f(W_t) - f(W_*))}, \end{aligned}$$

where the equalities are based on Lemma 1 and the second inequality is based on the fact that  $g(x) = \sqrt{x}$  is concave for  $x \geq 0$ . The last inequality is based on the properties of smoothness [Nesterov et al., 2018] and the fact that  $\|\cdot\|_{L^{-1}}$  is the dual norm of  $\|\cdot\|_L$ .

Then, for the variance part, let us first assume  $M = 1$  for simplicity, then we have

$$\begin{aligned} \mathbb{E} \left[ \left\| \left( \sum_{t=0}^{T-1} N_t N_t^\top \right)^{\frac{1}{2}} \right\|_* \right] &\stackrel{(10)}{\leq} \mathbb{E} \left[ \sqrt{\|V\|_* \operatorname{tr} \left( \left( \sum_{t=0}^{T-1} N_t N_t^\top \right)^{\frac{1}{2}} V^{-1} \left( \sum_{t=0}^{T-1} N_t N_t^\top \right)^{\frac{1}{2}} \right)} \right] \\ &= \mathbb{E} \left[ \sqrt{\|V\|_* \operatorname{tr} \left( \sum_{t=0}^{T-1} N_t N_t^\top V^{-1} \right)} \right] \end{aligned}$$

$$\begin{aligned}
&\leq \sqrt{\|V\|_* \sum_{t=0}^{T-1} \text{tr}(\mathbb{E}[N_t N_t^\top] V^{-1})} \\
&\leq \sqrt{\|V\|_* \sum_{t=0}^{T-1} \|V\|_*} = \sqrt{T} \|V\|_*,
\end{aligned}$$

where the equality is based on Lemma 1. and the second inequality is based on the fact that  $g(x) = \sqrt{x}$  is concave for  $x \geq 0$ . Then plugging these in Lemma 7, we have

$$\begin{aligned}
\frac{1}{T} \sum_{t=0}^{T-1} \mathbb{E}[f(W_t) - f(W_*)] &\leq \frac{D_{\text{op}}}{T} \mathbb{E} \left[ \left\| \left( 2 \sum_{t=0}^{T-1} \nabla f_t \nabla f_t^\top \right)^{\frac{1}{2}} \right\|_* \right] + \frac{D_{\text{op}}}{T} \mathbb{E} \left[ \left\| \left( 2 \sum_{t=0}^{T-1} N_t N_t^\top \right)^{\frac{1}{2}} \right\|_* \right] + \frac{\epsilon D_{\text{F}}^2}{D_{\text{op}} T} \\
&\leq \frac{2D_{\text{op}}}{T} \sqrt{\|L\|_* \sum_{t=0}^{T-1} \mathbb{E}[f(W_t) - f(W_*)]} + \frac{\sqrt{2} D_{\text{op}} \|V\|_*}{\sqrt{T}} + \frac{2\epsilon D_{\text{F}}^2}{D_{\text{op}} T}.
\end{aligned}$$

Thus if we denote  $x = \sqrt{\frac{1}{T} \sum_{t=0}^{T-1} \mathbb{E}[f(W_t) - f(W_*)]}$ , we can write the inequality as

$$x^2 \leq bx + c,$$

where

$$b = \frac{2D_{\text{op}} \sqrt{\|L\|_*}}{\sqrt{T}}, \quad c = \frac{\sqrt{2} D_{\text{op}} \|V\|_*}{\sqrt{T}} + \frac{\epsilon D_{\text{F}}^2}{D_{\text{op}} T}.$$

Then as  $x \geq 0$ , we can solve this simple quadratic inequality to obtain that

$$\begin{aligned}
x^2 &\leq \frac{1}{4} \left( b + \sqrt{b^2 + 4c} \right)^2 \leq 2b^2 + 2c \\
&\iff \frac{1}{T} \sum_{t=0}^{T-1} \mathbb{E}[f(W_t) - f(W_*)] \leq \frac{4D_{\text{op}}^2 \|L\|_*}{T} + \frac{2\sqrt{2} D_{\text{op}} \|V\|_*}{\sqrt{T}} + \frac{2\epsilon D_{\text{F}}^2}{D_{\text{op}} T},
\end{aligned}$$

which concludes the proof for  $M = 1$ . Then, based on Lemma 9 to incorporate batch size  $M > 1$ , we finish the proof.  $\square$

## G Proof of Section 6

Muon [Jordan et al., 2024] is essentially the following algorithm:

$$\begin{aligned}
B_t &= \mu B_{t-1} + G_t \\
U_t, S_t, V_t &= \text{Compact SVD}(B_t) \\
W_{t+1} &= W_t - \eta_t U_t V_t^\top,
\end{aligned} \tag{11}$$

where  $G_t$  is the gradient obtained at  $W_t$  and  $U_t \in \mathbb{R}^{m \times r_t}$ ,  $V_t \in \mathbb{R}^{r_t \times n}$  are the matrices of the  $r_t$  left and right singular vectors corresponding to the non-zero singular values of  $B_t$  that are the diagonal components of the diagonal matrix  $S_t \in \mathbb{R}^{r_t \times r_t}$  with  $r_t$  being the rank of  $B_t$ . Note that  $U_t S_t V_t^\top$  is referred to as the "compact" or "Reduced" SVD of  $B_t$ . Muon implements this algorithm using Newton-Schulz matrix iterations to approximately compute  $U_t V_t^\top$  instead of directly employing SVD to improve computational efficiency. The relationship between (11), with  $B_t = G_t$ , and (2) is interpreted in Bernstein and Newhouse [2024b] (see Story II). In the following discussion, we refer Muon as the one described in (11). We first show that ASGO and Muon, without gradient accumulation and momentum, are equivalent.

**Proposition 1.** *If in ASGO (Algorithm 2 version) we set  $\beta_1 = \beta_2 = 0, \epsilon = 0$ , and  $\tau = 1$ , and in Muon (11) we set  $\mu = 0$ , ASGO is equivalent to Muon.*

*Proof.* Let  $U_t S_t V_t^\top$  be the compact SVD of  $G_t$ . For ASGO, the update is

$$\begin{aligned}
W_{t+1} &= W_t - \eta_t (G_t G_t^\top)^{-\frac{1}{2}} G_t \\
&= W_t - \eta_t (U_t S_t S_t^\top U_t^\top)^{-\frac{1}{2}} U_t S_t V_t^\top \\
&= W_t - \eta_t U_t (S_t^2)^{-\frac{1}{2}} U_t^\top U_t S_t V_t^\top \\
&= W_t - \eta_t U_t S_t^{-1} S_t V_t^\top \\
&= W_t - \eta_t U_t V_t^\top.
\end{aligned}$$

Clearly, this is the same as Muon.  $\square$

We now prove a nonconvex convergence result for Muon in the deterministic case with  $\mu = 0$ .

**Theorem 4** (Nonconvex convergence of Muon). *We consider Muon presented in (11) with  $\mu = 0$ . In the deterministic case, i.e. no gradient noise, if we assume that there exists a lower bound  $f^*$  such that  $f(W) \geq f^*$  for all  $W$  and Assumption 2, by taking  $\eta_t \equiv \eta = \sqrt{\frac{2(f(W_0) - f^*)}{\|L\|_* T}}$ , it holds that*

$$\frac{1}{T} \sum_{t=0}^{T-1} \|\nabla f(W_t)\|_* \leq \sqrt{\frac{\|L\|_* (f(W_0) - f^*)}{2T}}.$$

*Proof.* Since we assume the deterministic setting, we have  $G_t = \nabla f(W_t)$ . Also, since we assume  $\mu = 0$ , we have  $U_t, V_t$  are the left and right singular vectors of  $G_t$  such that  $G_t = U_t S_t V_t^\top$ . Then based on the smoothness assumption, it holds that

$$\begin{aligned}
f(W_{t+1}) &\leq f(W_t) + \langle \nabla f(W_t), W_{t+1} - W_t \rangle + \frac{1}{2} \text{tr}((W_{t+1} - W_t)^\top L(W_{t+1} - W_t)) \\
&= f(W_t) - \eta_t \text{tr}(G_t^\top U_t V_t^\top) + \frac{\eta_t^2}{2} \text{tr}((U_t V_t^\top)^\top L(U_t V_t^\top)) \\
&= f(W_t) - \eta_t \text{tr}(V_t S_t U_t^\top U_t V_t^\top) + \frac{\eta_t^2}{2} \text{tr}(V_t U_t^\top L U_t V_t^\top) \\
&= f(W_t) - \eta_t \text{tr}(V_t S_t V_t^\top) + \frac{\eta_t^2}{2} \text{tr}(U_t^\top L U_t V_t^\top V_t) \\
&= f(W_t) - \eta_t \text{tr}(S_t V_t^\top V_t) + \frac{\eta_t^2}{2} \text{tr}(L U_t U_t^\top) \\
&\leq f(W_t) - \eta_t \|G_t\|_* + \frac{\eta_t^2}{2} \|L\|_*,
\end{aligned}$$

where the last inequality is because of the fact that  $U U^\top \preceq I$  and Lemma 1. Then by summing up over  $t$  and rearrangement, we can obtain that

$$\sum_{t=0}^{T-1} \eta_t \|G_t\|_* \leq f(W_0) - f(W_T) + \sum_{t=0}^{T-1} \frac{\eta_t^2}{2} \|L\|_*.$$

Then we take  $\eta_t \equiv \eta$  to obtain that

$$\frac{1}{T} \sum_{t=0}^{T-1} \|\nabla f(W_t)\|_* \leq \frac{f(W_0) - f^*}{\eta T} + \frac{\eta}{2} \|L\|_*.$$

Setting  $\eta = \sqrt{\frac{2(f(W_0) - f^*)}{\|L\|_* T}}$  finishes the proof.  $\square$